Article

A Comprehensive Analysis of Hurricane Damage across the U.S. Gulf and Atlantic Coasts Using Geospatial Big Data

Gainbi Park (ID)

Centre for Urban and Regional Development Studies (CURDS), School of Geography, Politics and Sociology, Newcastle University, Newcastle Upon Tyne NE1 7RU, UK; gainbi.park@newcastle.ac.uk

Abstract: (1) Background: Hurricane events are expected to increase as a consequence of climate change, increasing their intensity and severity. Destructive hurricane activities pose the greatest threat to coastal communities along the U.S. Gulf of Mexico and Atlantic Coasts in the conterminous United States. This study investigated the historical extent of hurricane-related damage, identifying the most at-risk areas of hurricanes using geospatial big data. As a supplement to analysis, this study further examined the overall population trend within the hurricane at-risk zones. (2) Methods: The Sea, Lake, and Overland Surges from Hurricanes (SLOSH) model and the HURRECON model were used to estimate the geographical extent of the storm surge inundation and wind damage of historical hurricanes from 1950 to 2018. The modeled results from every hurricane were then aggregated to a single unified spatial surface to examine the generalized hurricane patterns across the affected coastal counties. Based on this singular spatial boundary coupled with demographic datasets, zonal analysis was applied to explore the historical population at risk. (3) Results: A total of 775 counties were found to comprise the "hurricane-prone coastal counties" that have experienced at least one instance of hurricane damage over the study period. The overall demographic trends within the hurricane-prone coastal counties revealed that the coastal populations are growing at a faster pace than the national average, and this growth puts more people at greater risk of hurricane hazards. (4) Conclusions: This study is the first comprehensive investigation of hurricane vulnerability encompassing the Atlantic and Gulf Coasts stretching from Texas to Maine over a long span of time. The findings from this study can serve as a basis for understanding the exposure of at-risk populations to hurricane-related damage within the coastal counties at a national scale.

Keywords: hurricane damage; storm surge; wind damage; geospatial big data; hurricane-prone coastal counties; population vulnerability

1. Introduction

Hurricanes are extreme meteorological events that are likely to be affected by climate change, of which global warming and sea level rise are two foreseeable changes that could impact the consequences of hurricane disasters. The frequency and/or intensity of hurricanes are projected to increase in the coming decades, producing high-speed winds and heavy precipitation [1–5]. Hurricanes have historically proven to be some of the most devastating and costliest natural disasters in the Gulf of Mexico and Atlantic coast regions of the United States, having the highest average event cost (USD 21.5 billion per event), and causing the highest number of fatalities (6593) and the largest economic losses (USD 945.9 billion total of all natural disasters between 1980 and 2020) [6–8]. The primary causes of the massive damage and loss of life are storm surge flooding and high-speed winds. In particular, drownings from storm surges are responsible for most hurricane-related casualties and injuries [9–12].

U.S. coastal populations are already experiencing the risk of hazards such as hurricanes, storm surges, sea level rise, and coastal erosion. The fast-growing coastal population and demographic shifts along the coastal regions are playing a major role in substantially

aggravating the consequences of hurricanes [2,13–15]. Approximately 123.3 million people, which amounts to 39% of the total U.S. population, resided in hurricane-prone coastal areas in 2010, increasing to 127 million people in 2016. The population was expected to grow to 134 million (i.e., an 8% increase) from 2010 to 2020 in coastal zones. Coastal populations are projected to increase up to 144 million people (i.e., 20% increase) by 2025 within 100 km of the coastal areas in the United States, thereby continuously increasing coastal populations' vulnerability to natural hazards [16,17].

Increasingly destructive hurricane activities pose a threat to these coastal communities along the U.S. Gulf of Mexico and Atlantic coasts. Rapid coastal population growth puts more people in harm's way, and rising property values by accelerating urbanization and intensive development have placed more environment-related stresses on coastal areas. The burgeoning coastal settlement and coastal-dependent economic activities (e.g., shipping, tourism, fisheries, and petroleum industry) are attracting more people to move to the hurricane coasts [13,14]. Specifically, the Gulf of Mexico regions have seen an 8.5% increase in population employed in construction industries and a 10.8% increase in employment in maintenance occupations, which is higher than the national rate [18]. Overdevelopment due to the high demand for second homes and coastal real estate has increased the risk and exposure of people and infrastructure to hurricane-related damage more than ever before [2,13,19–21].

Estimating exposure to hurricane risk is a fundamental step in comprehending the geophysical vulnerability of coastal populations [22]. Most research investigating hurricane hazards has been largely based on various hydrodynamic models such as the Sea, Lake, and Overland Surges from Hurricanes (SLOSH), H*Wind (hurricane wind analysis system), or Simulating WAves Nearshore (SWAN) coupled with ADvanced CIRCulation (ADCIRC) models. Each of these models requires a unique set of parameters using different wind model equations and have their strengths and weaknesses [11,23–26]. The majority of the existing literature applies these models in the field of coastal engineering and atmospheric research. Recently, an R package called "stormwindmodel" simplified the complicated modeling procedure for Atlantic Basin tropical storms, allowing researchers to facilitate rapid application for hurricane exposure assessment [27,28].

To date, numerous studies have assessed hurricane vulnerability on a case-by-case basis, focusing on the most devastating hurricane events that have caused enormous societal losses. Such case-specific studies do not necessarily show the long-term effects of hurricane risks in coastal regions and provide a limited picture in assessing the comprehensive vulnerability to hurricane hazards over time. This brings into question the spatial patterns of cumulative hurricane-related damage (particularly storm surge and wind-induced damage) based on past and recent hurricane events and their consequential effect on coastal population growth in hurricane-prone areas in the United States. The definition of "hurricane-prone region" has been restricted to flooding hazards in the current literature, which impedes the implementation of comprehensive hurricane vulnerability assessment using demographic datasets. One longitudinal study by Logan and Xu (2015) modeled hurricane-related hazards to capture spatial patterns of actual hurricane exposures that occurred from 1950 to 2005 [29]. Despite the importance of long-term research in hurricane vulnerability, there remains a paucity of longitudinal studies that systematically examine long-term trends of populations at increased risk of hurricane damage.

The objective of this study is therefore to estimate the geographic distribution of hurricane-related damage that has occurred in the United States throughout its history by modeling storm surge and wind damage. Specifically, this research is designed to answer the following research questions: (1) What are the spatial extent and intensity of storm surge inundation and wind damage caused by hurricanes along the Gulf and Atlantic coasts in the United States from 1950 onwards? (2) What regions have been particularly hard hit by hurricanes in the U.S. coastal counties over the past decades since 1950? (3) How has the overall population changed within the U.S. hurricane coastal counties over time? The increased risk of hurricane hazards has the potential to impact populations and residential

infrastructure within at-risk areas, making it essential to identify the areas with greater hurricane exposure. Hurricanes can negatively affect individuals and local communities through economic losses and infrastructure damage, among other ways. However, this study limits the scope to estimate the potential biophysical vulnerability of hurricanes through the estimation of historical hurricane damage at the national level. The social and economic consequences of hurricane damage on society are broadly defined, and thus consideration of these various sectors lies beyond the scope of this study.

The remainder of this paper has been divided into four sections. Section 2 provides a brief overview of the study area, datasets, and methods adopted in the analysis. The coastal areas impacted by storm surge inundation and wind damage are presented at the national level in Section 3. In addition, this section also shows the total populations that have been exposed to hurricane-related damage during the study period. Section 4 presents the conclusions, significance, and limitations of this research that can be further investigated in the future.

2. Materials and Methods

2.1. Modeling Large-Scale and Long-Term Historical Hurricanes

Vulnerability science has been extensively applied to a wide variety of academic fields such as ecology, public health, sustainable science, environmental justice, and disaster risk management [30]. The question is what exposes people and places to greater harm from environmental hazards? Within risk, hazard, and disaster scholarship, vulnerability science has long encompassed three different but intersecting domains: physical/natural systems (e.g., exposure, intensity, frequency of occurrence), human systems including social systems and built environment (e.g., socio-demographic characteristics of at-risk populations, the degree of urbanization), and local spatial characteristics of places (e.g., location-specific conditions such as proximity to hazardous areas) [31,32]

With the abundance and increasing accessibility of georeferenced big data, vulnerability and environmental sciences are evolving to incorporate new methodologies to handle increasingly complex datasets that describe the complexity of human–environment interactions and the dynamic characteristics of natural hazards [33]. This era of big data has led to advances in vulnerability research in estimating, predicting, and visualizing potential risk or vulnerability to natural hazards using large volumes of data and a variety of data-driven computing approaches [34–37]. Big data can be defined in a variety of ways depending on the disciplines and subjects being studied. However, there are three components that can be considered the fundamentals of big data termed the "three Vs": (1) volume—the quantity of data that are collected, stored, and processed; (2) velocity—how fast the data are collected and processed; and (3) variety—the types/sources of data [38–40]. This study aimed to highlight the usefulness of the longest track records of the Atlantic hurricane public database in tandem with multiple geospatial data and hurricane modeling techniques in order to identify the most vulnerable areas to hurricanes in a spatially explicit manner.

There has been limited analysis of longitudinal hurricane-related damage in geographic scholarship that applies a variety of geospatial datasets and hurricane modeling techniques. Identifying the spatial extent of historical hurricane damage is crucial to examine the evolving physical and social vulnerability within the at-risk zone. For the purpose of comprehensive vulnerability assessment, this study provides a synoptic view of hurricane vulnerability in the United States on a large geographic scale using storm surge and wind damage modeling for a long period of time (1950–2018) at the national level. The current study does not incorporate inland flooding due to heavy rainfall, since this study relies on the accumulated hurricane events, not a single hurricane event.

Since historical geospatial data of hurricane impacts are seldom available, it is necessary to reconstruct to what extent past and recent hurricanes have affected coastal regions. Figure 1 shows the trajectories of all hurricanes and tropical storms that reached the U.S. East Coast, Florida, and Gulf Coast area during the study period. The hurricane-affected areas are nationwide, and states bordering the Gulf of Mexico and Atlantic Ocean have

borne the brunt of the catastrophic hurricane damage [13]. To reflect the full areal extent of the U.S. hurricane coasts, this study includes all hurricanes that made landfall along the Gulf and Atlantic Coasts up until 2018, encompassing a total of 22 states and the District of Columbia. This extensive hurricane modeling is in line with the three Vs of geospatial big data analytics.
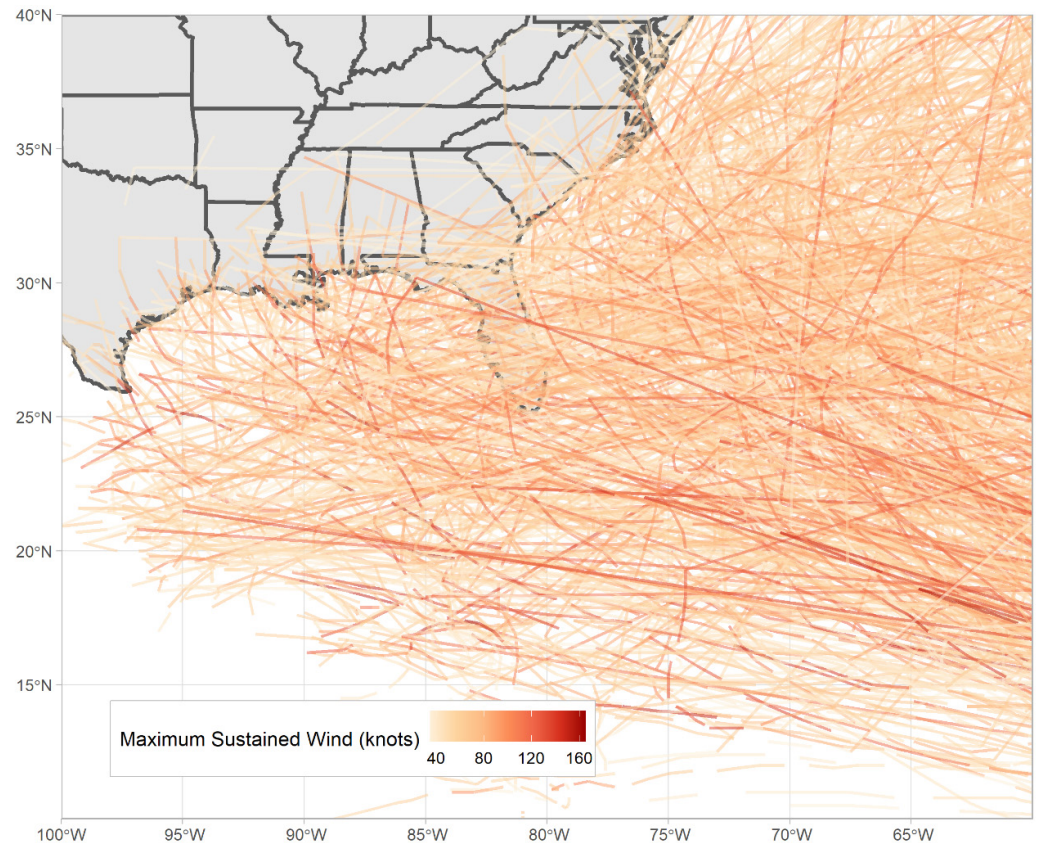

Figure 1. Historical hurricane and tropical storm tracks along the U.S. Gulf and Atlantic Coasts from 1950 to 2018.

The major data source of this hurricane-related damage modeling is the public Hurricane Database (known as the revised Atlantic hurricane database, HURDAT2). The HURDAT2 is the second-generation hurricane database maintained and updated annually by the U.S. National Oceanic and Atmospheric Administration (NOAA) at the National Hurricane Center (NHC). This dataset can be obtained from the NHC Data Archive (https://www.nhc.noaa.gov/data/, accessed on 1 October 2021), and it contains the best-estimated track records of all historical hurricanes, tropical storms, and subtropical storms of the Atlantic Basin, including the Gulf of Mexico and Caribbean Sea, since 1851 [41,42]. The HURDAT database provides a sufficient temporal resolution with position estimates for every synoptic time (0000, 0600, 1200, and 1800 UTC), and this allows researchers to capture the progress of each storm. Figure 2 presents the synoptic points of all hurricanes and tropical storms in the North Atlantic from 1851 to 2018. Each storm can be identified by its name and identifier number with its six-hourly information on date, time, position that geocodes the center of the storm (latitude and longitude), intensity (i.e., maximum sustained wind in knots), central pressure, and size [41–43]. These parameters are used to compute the storm surge heights and wind damage resulting from hurricanes by considering hurricane gust factors.
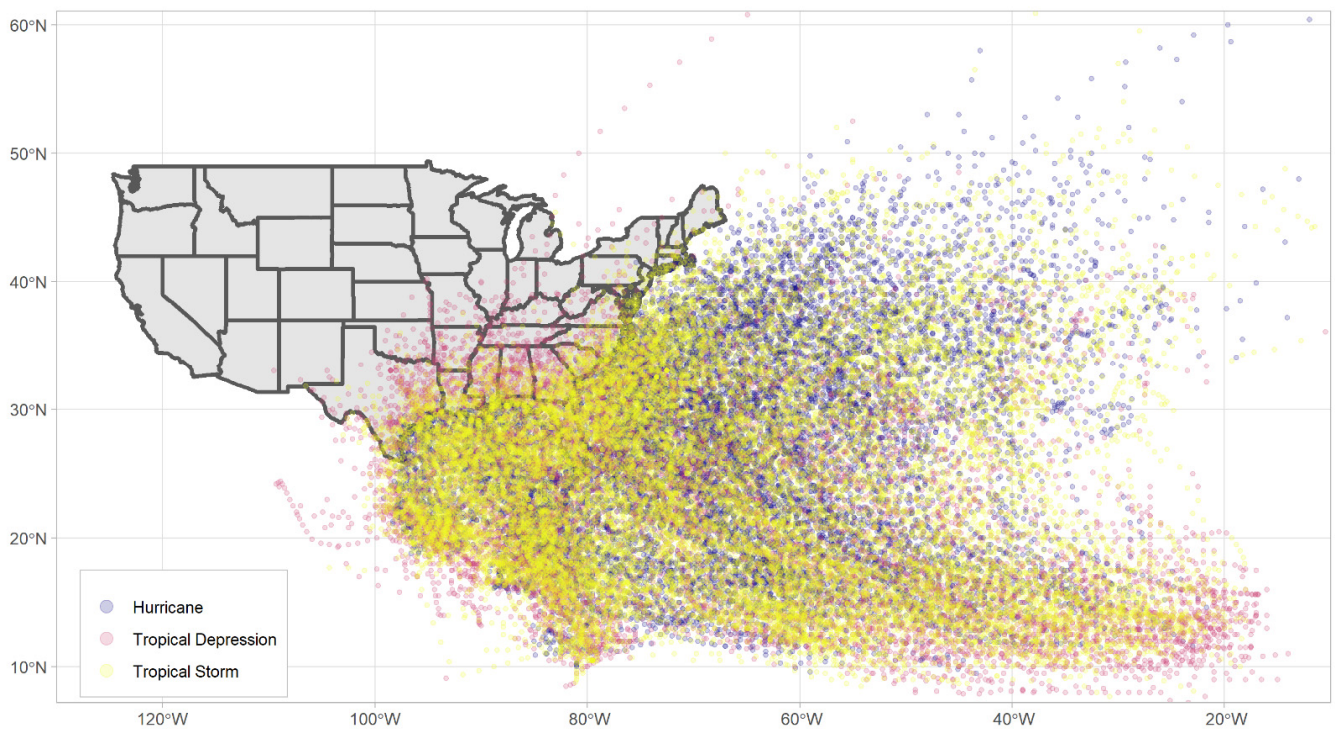
Figure 2. Synoptic data points of historical hurricanes (1851–2018) of the United States.

Oceanographic and atmospheric conditions also come into play in modeling the water surface caused by hurricanes and storms [44]. Topographic data or digital elevation models (DEM) are crucial in determining storm surge inundation because the shape of the terrain is highly related to how water flows and drains along and off a surface. The primary dataset used in this study was the U.S. Geological Survey (USGS) National Elevation Dataset (NED), which includes seamless elevation data covering the conterminous United States at different spatial resolutions [45]. In this study, the 1/3 arc-second (approximately 10 m) DEM dataset was selected for coastal inundation mapping and can be acquired from the USGS National Map Viewer.

Astronomical tidal information is also required to generate a water surface as an input value in storm surge modeling. The geographic location of tide level stations can be found at the NOAA Tides and Currents website. The SLOSH display program was then used to retrieve the initial water level (i.e., astronomical tide) for each hurricane at the nearby tide gauge station referring to the hurricane path observed 18 h before nearest approach (or landfall) in most storm situations. It is noteworthy to mention that the SLOSH model adopts National Geodetic Vertical Datum of 1929 (NGVD 29) as its vertical datum, meaning it is imperative to transform tidewater level to NGVD for consistent and reliable modeling results [29,46,47]. The description of the main attributes and software information employed in this study is summarized in Table 1.

Table 1. Geospatial data and software used in this study for hurricane modeling.

Data	Description	Data Source
Atlantic Hurricane Database (HURDAT2) 1851-2018	This dataset contains six-hourly information on the location, maximum winds, central pressure, and (starting in 2004) size of all known tropical cyclones and subtropical cyclones.	National Oceanic and Atmospheric Administration (NOAA) National Hurricane Center (NHC) https://www.nhc.noaa.gov/data/ (accessed on 1 October 2021)
SLOSH Basins (*.shp files)	The SLOSH basins are hyperbolic, elliptical, or polar mesh grids that are required to model storm surge heights. The spatial coverage of this study is the entirety of the U.S. Gulf and Atlantic Coasts.	SLOSH Display Program
SLOSH Display Program (SDP)	This program was used to download SLOSH basins and to visualize the results of the SLOSH model. Please note that the SLOSH model and the SLOSH Display Program (SDP) are two different tools. The SDP Tide information was also used to retrieve the astronomical tide data.	NOAA Slosh Display Package Webpage, https://slosh.nws.noaa.gov/sdp/ (accessed on 1 October 2021)
SLOSH Model	This is a computer model used by the National Hurricane Center to forecast and simulate storm surge vulnerability caused by historical, hypothetical, or predicted hurricanes.	Available to interested users upon request to NOAA
Tide level station	The SLOSH model requires the observed coastal sea levels within a basin.	NOAA Tides and Currents, https://tidesandcurrents.noaa.gov/ (accessed on 1 October 2021)
VDatum	This software is a conversion tool for converting initial water heights between vertical datums—tidal, orthometric, and ellipsoidal datums.	NOAA Vertical Datums Transformation, https://vdatum.noaa.gov/ (accessed on 1 October 2021)
Corpscon 6.0	This software was used to transform the vertical datums of SLOSH modeling outputs (NGVD 29) to the reference vertical datum (NAVD 88).	US Army Corps of Engineers Geospatial Center, https://www.agc.army.mil/What-we-do/Corpscon/ (accessed on 1 October 2021)
National Elevation Dataset (NED)	The 1/3 arc-second DEM dataset with full coverage of coastal counties was used to create the inundation extent and depth.	U.S. Geological Survey (USGS) National Map Viewer, https://apps.nationalmap.gov/viewer/ (accessed on 1 October 2021)
Land use/land cover (LULC)	The National Land Cover Database (NLCD) was used to calculate the developed areas within the hurricane-affected areas in estimating at-risk populations in Section 3.2. Non-developed areas were masked out from the NLCD datasets for the hurricane-affected areas.	Multi-Resolution Land Characteristics Consortium, https://www.mrlc.gov/ (accessed on 1 October 2021)
HURRECON	This software estimates wind speed, wind direction, and wind damage on the Fujita scale for a single or multiple hurricanes in a given region. The input parameters (hurricane track and intensity information) can be acquired from the HURDAT2 database. HURRECON is available in both R and Python.	Environmental Data Initiative Data Portal, https://doi.org/10.6073/pasta/0878074e6c87ec8b43cb56601ff00472 (accessed on 1 October 2021) or GitHub https://github.com/hurrecon-model/HurreconR (accessed on 1 October 2021)

2.2. Methods

The majority of damage and loss of life are associated with storm surges and high winds in the wake of hurricanes, and impacts have been unevenly distributed across the U.S. during the past several decades. This study intended to determine the geographic extent of storm surges and wind damage over an extended period of time from

1950 to 2018 to identify the comprehensive locational vulnerability to hurricane impacts. Figure 3 represents the methodological procedures used to obtain an estimate of the overall hurricane-related damage.
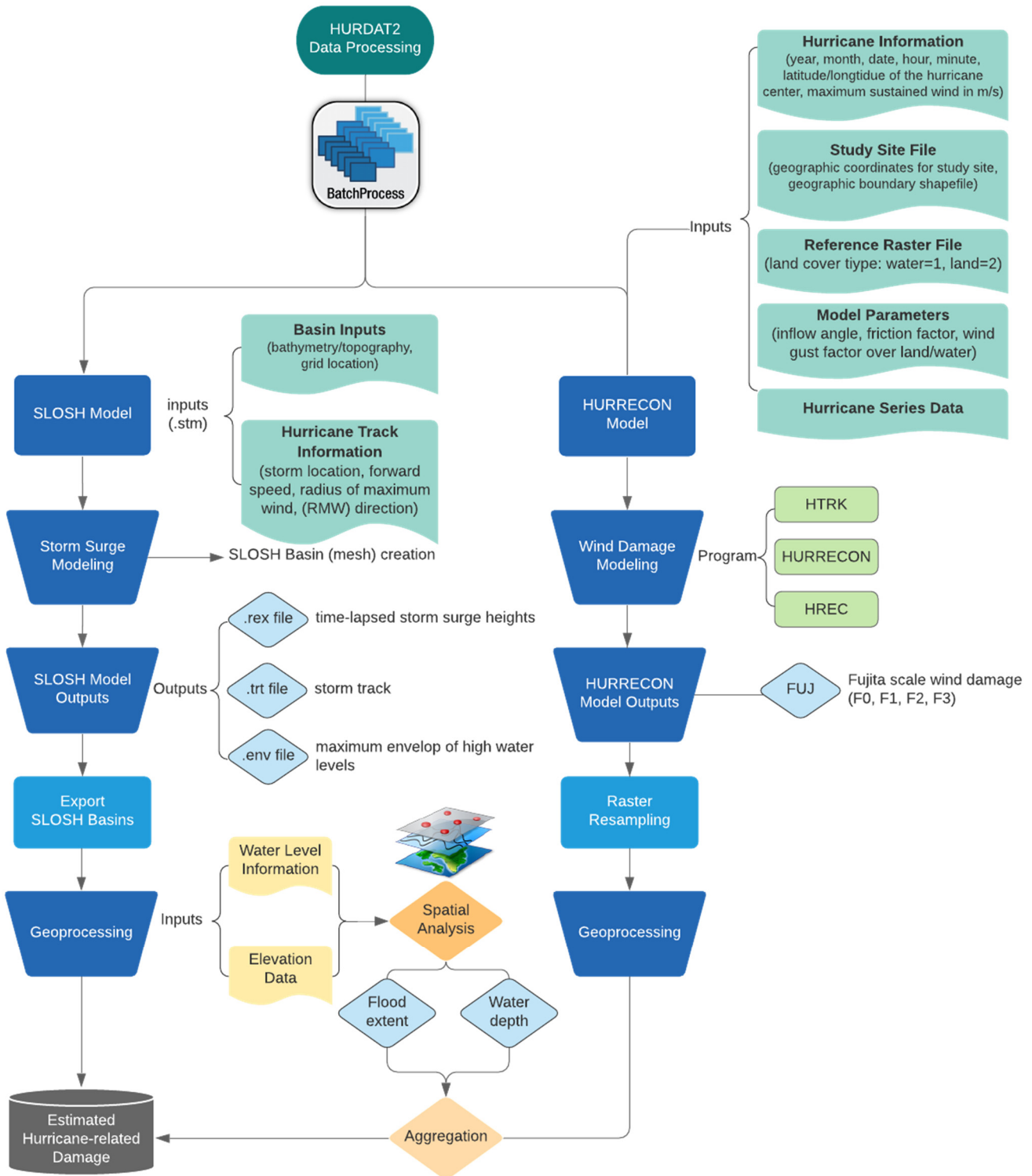

Figure 3. Flowchart for comprehensive hurricane-related damage modeling.

2.2.1. Estimation of Storm Surge Inundation

In an attempt to overcome data scarcity in historical GIS hurricane data, this study adopted a hydrodynamic model, called the Sea, Lake, and Overland Surges from Hurricanes (SLOSH) model, in obtaining the spatial extent and intensity of storm surges. The SLOSH model was used to simulate the storm surges induced by each track over the study period. The SLOSH model is currently being used by the NHC for real-time forecasting of potential hurricane storm surges across the entire seaboard of the United States [10,11,46]. A major advantage of the SLOSH model is its ability to reproduce historical hurricane storm surges based on the HURDAT2 dataset [23,46,48].

The SLOSH model is a two-dimensional numerical coastal model that computes the maximum water heights considering the dynamic flow of water over land and water based on pre-determined grid cells referred to as a basin. Currently, there are 32 basins covering the entirety of the U.S. Atlantic and Gulf of Mexico Coasts, Hawaii, Puerto Rico, Virgin Islands, and the Bahamas (Figure 4). All hurricanes and tropical storms that made landfall along the coastal regions can be modeled with the operational SLOSH basins. If a hurricane impacted a larger extent of the area, multiple basins were considered in the modeling procedure. Depending on the region, the basins have different shapes (mostly polar or hyperbolic/elliptical) composed of thousands of grid cells, and these are one of the primary inputs of the meteorological parameters that must be entered in the modeling process [49]. The closer to the primary area of interest such as a bay or a region immediately adjacent to the coastline, the finer the resolution of the grid cells. Meanwhile, the spatial resolution of the grid cells is coarser in the deep open oceans due to a low significance in simulation. The basins integrate geographical characteristics of the particular area along the coasts that influence storm surges such as topography, shoreline structure, levees, bathymetry of ocean areas, and continental shelves [23,50]. The accuracy of the estimated surge height is known to be within $\pm 20\%$ of the observed water heights. The model uncertainties can be attributed to several components such as the basin's spatial resolution, vertical accuracy of terrain data/high water marks, and the meteorological/geophysical parameters resulting from the complexity of hurricane and astronomical tides [10,44,51].

The left side of Figure 3 depicts the overall procedure of storm surge simulation. Modeling storm surges requires the following meteorological parameters as input parameters to generate the wind field that drives the storm surge inundation: storm track positions (i.e., latitude and longitude at 6-h intervals), intensity (i.e., storm central pressure at 6-h intervals), radius of maximum wind (RMW, i.e., size—the distance between the center of a storm and the location where the strongest wind is generated, at 6-h intervals), forward speed, and landfall time [46,52]. The stm.file consists of 13 time points of these input parameters for model operation to describe an hourly progression of the hurricane before and after landfall. Considering these input parameters coupled with a selected basin, the SLOSH model can determine the flow of storm surges across the surface and then estimate the maximum envelope of water in each basin grid during a storm's life cycle.

The outputs of the SLOSH model consist of three files: (1) the *.rex file is a time-lapsed animation file that contains the simulated water levels at every grid cell over the duration of the storm; (2) the *trt.file is an expansion of the stm.file providing hourly values, resulting in 100 h of input data; and (3) the *.env.file provides the envelope of high water levels. The .rex file can be converted to a shapefile for additional geoprocessing. The SLOSH model does not include the wave components (i.e., astronomical tides or wind-driven wave heights) and antecedent precipitation on top of the surge, and thus the astronomical tides can be added to the model results [10,29,53–55]. As a result, the SLOSH model generates time-dependent storm surge water levels at every grid cell at a specific interval of time at each basin. As an example, Figures 5 and 6 show a simulated storm surge height during Hurricane Harvey (2017) based on the SLOSH simulation. The resulting individual storm surge output was compared with the existing SLOSH model from NOAA. The interpolated raster for each hurricane can be further analyzed to generate the final layer that represents the extent of inundation and the flood depth by adding the astronomical tides.

Spatial analysis can be conducted to derive the inundation extent and the depth of a storm surge using the simulated water height from the SLOSH model and DEM data. The maximum surge water height generated from the SLOSH model can be converted to a GIS file format to create centroids of SLOSH basin outputs and then interpolate water level heights using the natural neighbor method. It is important to note that each dataset refers to a different vertical datum: the SLOSH model output references the National Geodetic Vertical Datum of 1929 (NGVD29); the initial tidewater level refers to mean lower low water (MLLW); the elevation data are based on the North American Vertical Datum of 1988 (NAVD88). All elevations are based on different vertical datums and cannot be directly used to compute storm surge heights. Therefore, it is required to maintain a consistent vertical datum between the estimated storm surge inundation height and the terrain elevation data using a transformation to derive the depth of a storm surge accurately. In this study, Corpscon, Version 6.0 was utilized to conduct vertical conversions between the NGVD 29 and the NAVD 88. To process large amounts of GIS datasets and vector- and raster-based analysis, this study employed batch processing using ArcGIS and R in conjunction.

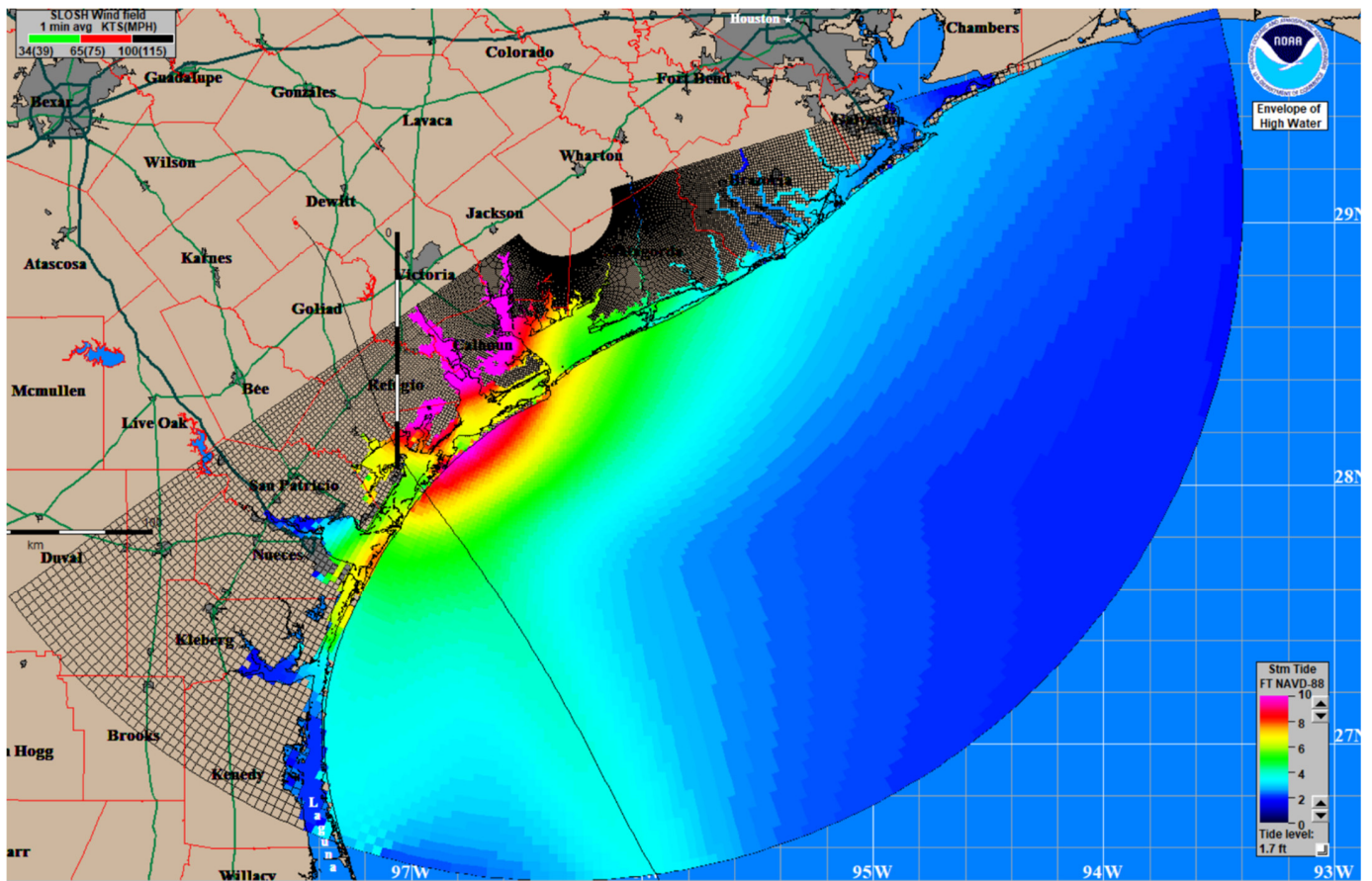**Figure 4.** The spatial extent of operational basins (or grids) in the SLOSH model.

Figure 5. Hurricane Harvey (2018) storm surge heights simulated by the SLOSH model in the Matagorda Bay (ps2) basin.
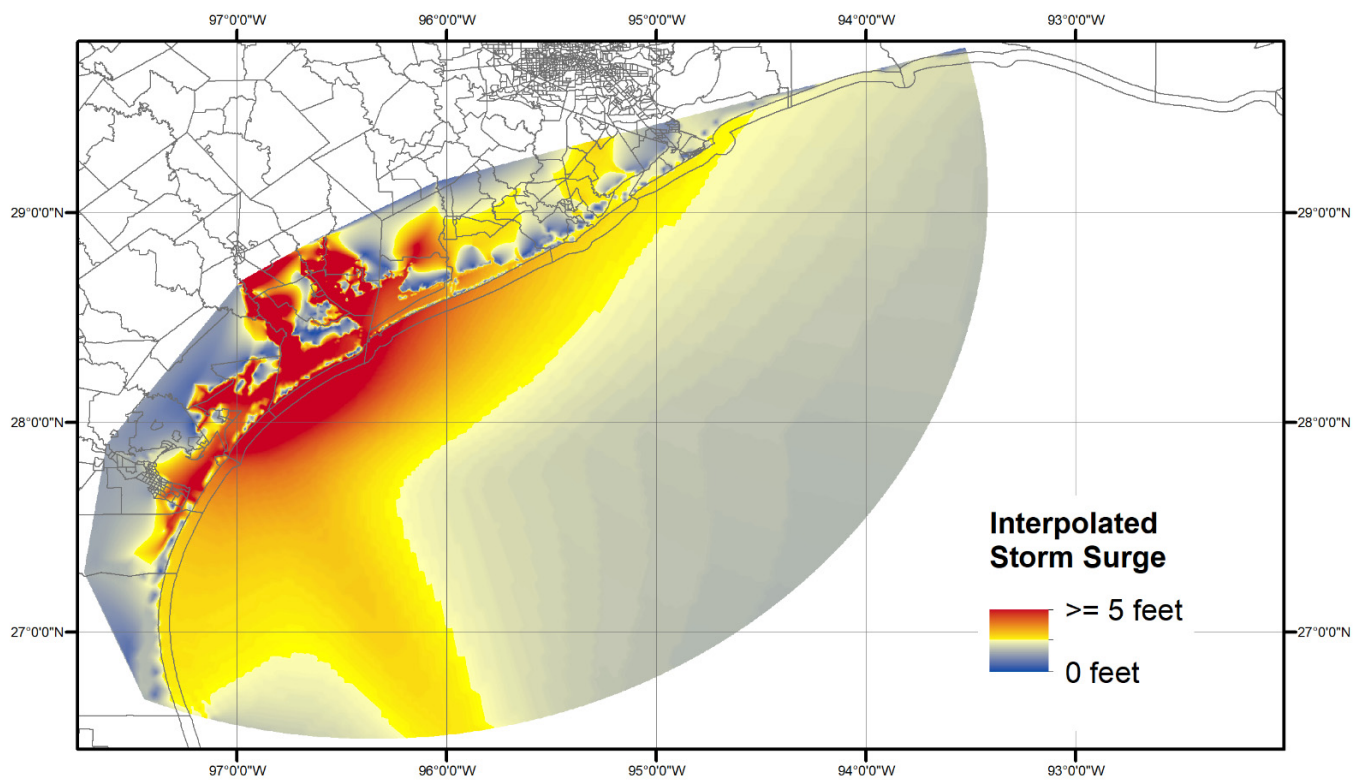

Figure 6. Interpolated storm surge inundation (before conducting additional geoprocessing operations) from Hurricane Harvey (2017).

2.2.2. Estimation of Wind Damage

Strong hurricane winds often cause severe structural damage to infrastructure, residential structures, and commercial structures [21]. This study adopted a meteorological model, HURRECON (Hurricane Reconstruction), which is based on published empirical studies of hurricanes in the New England, Puerto Rico, and Gulf Coasts [29,56,57], in order to reconstruct the intensity of wind damage by each hurricane. The HURRECON model was developed to estimate the basic structure of a storm's surface wind conditions such as sustained wind velocity, peak gust velocity, and wind direction of movement over a specified surface cover type (water and land). It has been widely applied to study the impact of hurricane wind disturbance on forestry landscapes [56–58] and hurricane wind damage assessment [29,59].

As described on the right side of Figure 3, the HURRECON model also uses the meteorological parameters of a storm (i.e., storm track and wind speed) from the HURDAT2 database as input data. The individual hurricane position data (*.pos file, a tab-delimited text file) should contain year, month, day, hour, minute, latitude/longitude, and maximum sustained wind in meters per second (m/s). The model also requires a rectangular geographic file (i.e., 16-bit IDRISI raster file format) to distinguish the land cover type (water or land) in estimating the surface wind speed and direction. The raster grid should be equally divided per cell to produce a more accurate modeling result. The parametric equations are well documented in the literature [29,56,57,60]. The HURRECON model can be implemented in a series of separate programs. First, the HTRK program can be run to create a track file of interpolated input parameters. Next, the HURRECN program can be utilized to estimate wind velocity and direction for a given geographic location. The output from the HURRECON program can then be operated to convert the outputs to Fujita scale damage (Figure 7).
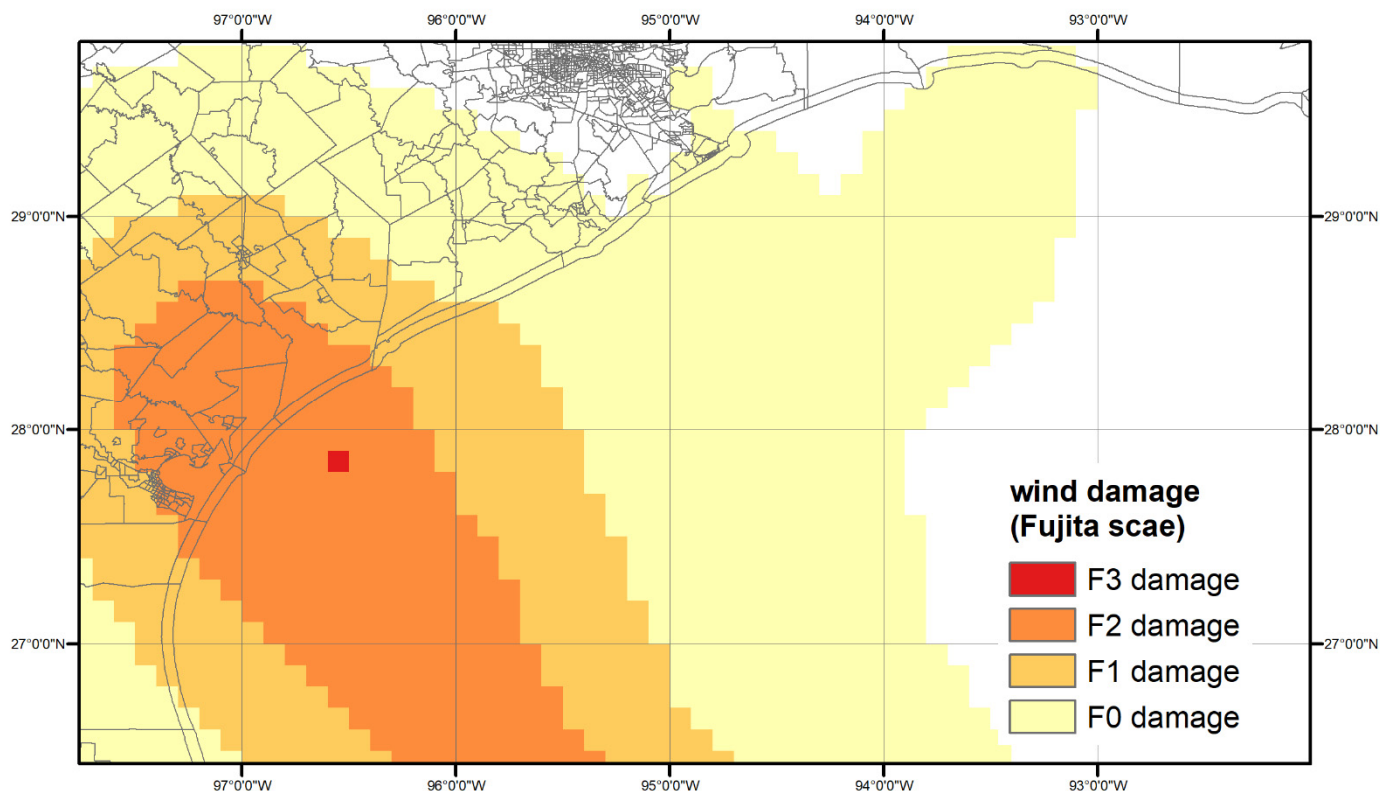

Figure 7. Simulated wind damage by Hurricane Harvey (2017) using the HURRECON model.

In this model, the predicted wind damage is adjusted for hurricane wind field estimation and then classified into the modified Fujita scale classes (no damage, F0, F1, F2,

F3)—originally proposed by Fujita [61] to characterize the wind intensity and damage by tornadoes—by correlating the maximum quarter-mile wind speed with wind damage intensity [56,57,60,61]. The original F-scale (Fujita scale) was devised to assess and categorize actual wind damage by its intensity and area on a wind speed scale, ranging from F0 (light damage in gale-force wind) to F5 (incredible damage). It has been utilized by the U.S. National Weather Service for tornadoes and hurricanes since the 1970s. The F-scale has been recently updated with the improved scale, called the Enhanced Fujita (EF) scale, based on a rating of tornadoes but not applicable to hurricane intensity [62,63]. In response to this, Boose, Foster, and Fluet [60] developed a modified F-scale rating tailored to hurricane damage levels. This modified F-scale was used in this study as opposed to the Saffir–Simpson scale in order to adhere to the model specifications of the HURRECON model.

The modified F-scale was extended to reveal widespread exterior structural damage by hurricane-force wind to buildings, (e.g., damaged roof shingles, broken windows or chimneys, and destruction of buildings), vehicles/infrastructure (e.g., unrooted traffic lights or utility poles, destroyed roads and rails), and the natural environment (e.g., blown down trees). It is ranked on an ordinal scale (F0, F1, F2, and F3) based on sustained wind speed and its corresponding post-hurricane damage level: F0 = 18–25 m/s (minor damage to buildings/trees), F1 = 26–35 m/s (houses unroofed or damaged, and single or isolated groups of trees blown down), F2 = 36–47 m/s (houses unroofed or destroyed and extensive tree blowdowns), and F3 = 48–62 m/s (houses blown down or destroyed, most trees down, and heavy automobiles lifted or overturned). The F-scale is beneficial for broad applications and can be universally applied across regions, since it does not rely on construction practices in a particular area in the United States, such as the International Building Code (IBC) or International Residential Code (IRC) [64].

The HURRECON model can generate the prediction of wind damage for an individual site as a table or for the entire area of interest as an IDRISI raster format (16-bit), which is compatible with TerrSet Geospatial Monitoring and Modeling software (formerly IDRISI). It is required to convert the raster outputs to 32-bit raster images using resampling techniques to be displayed in ArcGIS software. The predicted wind damage by Hurricane Harvey is shown in Figure 7 as an example. The original HURRECON model was written in Pascal language coupled with IDRISI. The model has recently been updated in both the R (HurreconR) and Python (HurreconPython) packages for operating system compatibility, and these packages are available in public repositories of GitHub (https://github.com/hurrecon-model/HurreconR, accessed on 1 October 2021).

The HURRECON model is subject to certain limitations. First, it does not consider non-meteorological factors that could affect wind damage at the local level such as construction materials of residential/commercial buildings, building code changes, and topographic effects. Hence, the results from the model cannot be interpolated to the local level or small geographical areas (e.g., census tracts or Census Block Groups) [29]. Second, the estimated wind model does not take into account the antecedent precipitation, lacking the capacity to model the impact of inland flooding. Given the unit of analysis being studied for wind damage assessment, the model outputs still produce reasonable estimation in spite of its limitations.

3. Results

3.1. Cumulative Hurricane Risk

The modeled results from every hurricane were aggregated to a single unified spatial surface, reflecting the long-term hurricane impacts across the entire coastal areas for decades. The resultant unified geographic extent of all hurricane-related damage is based on 190 hurricanes and tropical storms during the study period from 1950 to 2018, serving as a baseline to examine at-risk populations to hurricane-related damage along the coastal counties in the following section.

Figure 8 represents the coastal regions that have been exposed to the impact of one foot or higher of storm surge since 1950. The result is consistent with the NOAA/National

Weather Service/National Hurricane Center Storm Surge Unit's storm surge inundation map [45]. Storm surge damage is highly localized along coastal areas. Overall, a stretch of the Gulf Coast from South Texas to the Florida Panhandle has borne the brunt of storm surge damage over time. Southeastern Louisiana (especially the Lower Mississippi River Delta region), Alabama, Mississippi, and the northwestern Panhandle of Florida have been hard hit by the most intensive storm surges more than twenty-one times, with the maximum frequency of thirty-nine for the past several decades. Western Louisiana, Southwestern Florida, and West Central Florida have also experienced frequent exposure to storm surge impacts. In the southeastern coastal regions, the Charleston area in South Carolina, the Outer Banks, and the coastal counties near Brunswick, New Hanover, Pender, and Onslow Counties have been affected by storm surges at least eleven times. In contrast, the Mid-Atlantic region has been relatively less affected by storm surge inundation. In particular, the Chesapeake Bay area—especially the southeastern shore of Virginia (Hampton Roads region) and the southern tip of the Delmarva Peninsula—has been flooded by storm surges at least ten times. It is not unusual to observe fairly frequent storm surge inundation in the Eastern Long Island regions (Nassau and Suffolk Counties) and southwestern Connecticut. New England regions have also been subject to coastal inundation for decades. These regions are increasingly becoming more susceptible to hurricane strikes due to climate change and sea level rise [13,65,66].
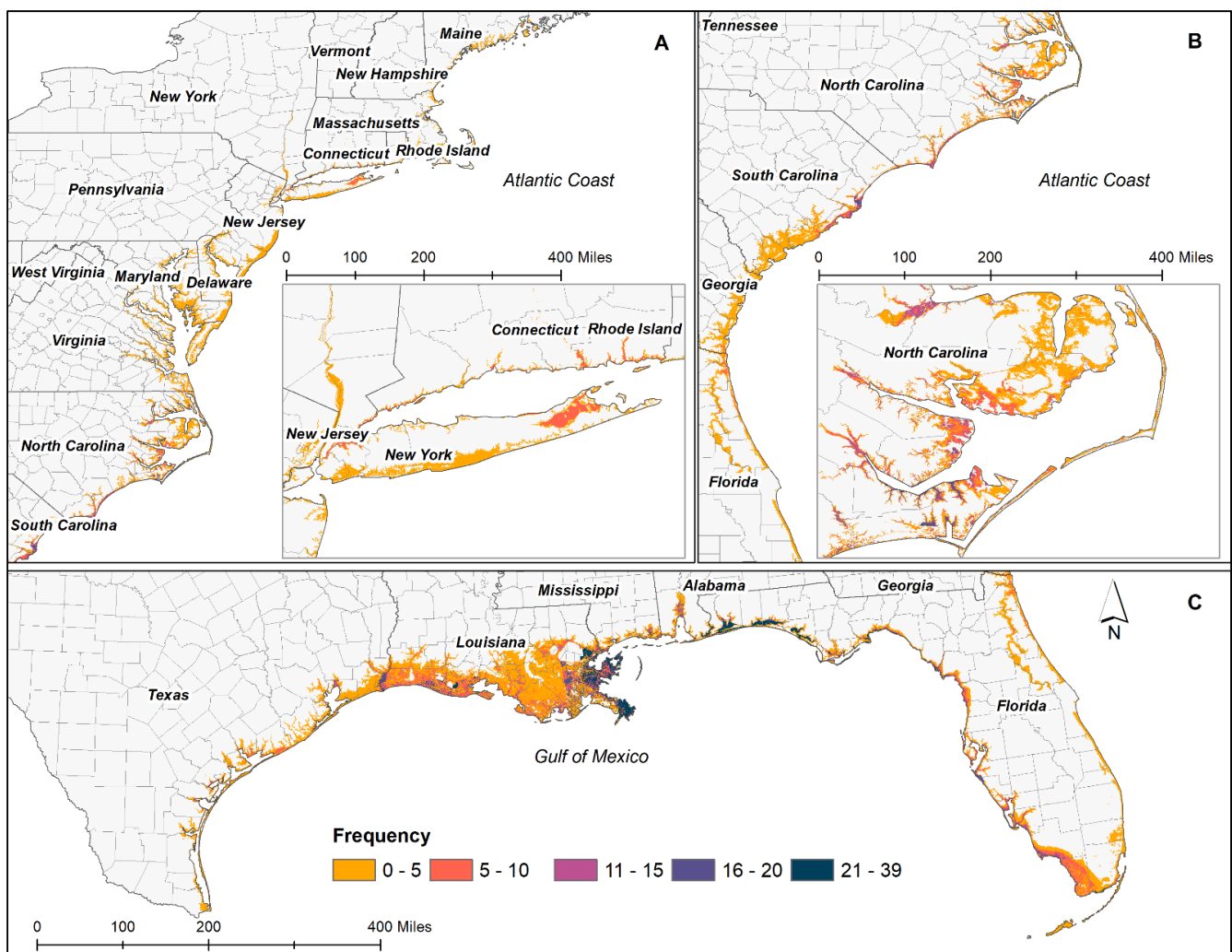
Figure 8. Modeled frequency of storm surge inundation of one foot or higher based on hurricanes: (**A**) The Northeast region; (**B**) The Southeast region; and (**C**) The Gulf Coast region.

The HURRECON-modeled results were compiled to show a more complete picture of wind damage for the entirety of the coastal regions on the Fujita scale since 1950 (Figure 9). As hurricanes make landfall along the coast, wind speeds rapidly weaken due to the higher frictional effects of land surfaces and a lack of moisture and latent heat energy from the ocean [67]. Occasionally, hurricanes can travel hundreds of miles deep into the interior counties after landfall, intensifying their power. Hence, the areas affected by hurricane winds are not just limited to the immediate vicinity of coastal regions but also areas further inland.
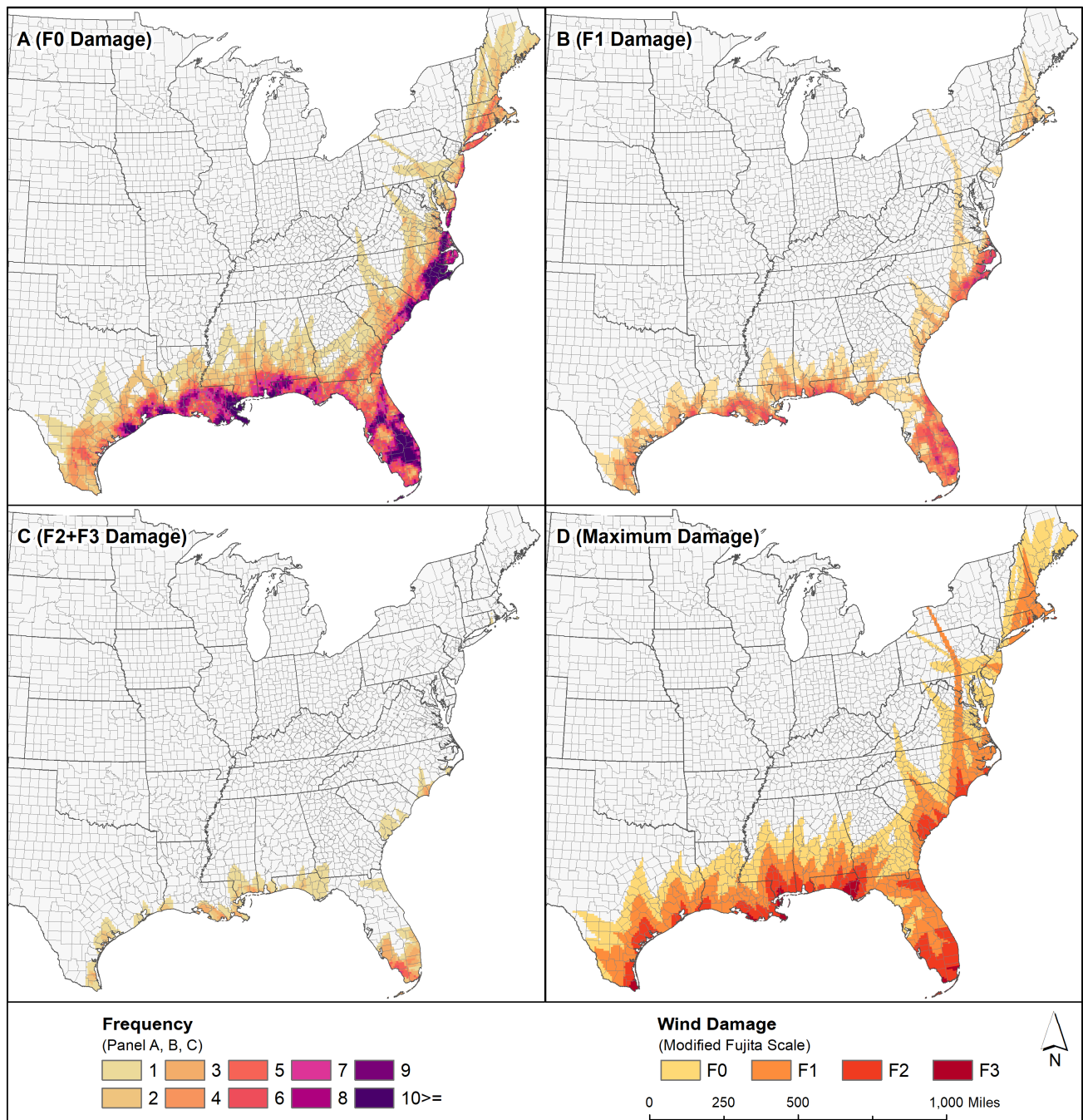
Figure 9. Modeled wind damage frequency and intensity from 1950 to 2018: (**A**) the spatial extent of F0 wind damage (minor damage to buildings/trees); (**B**) F1 wind damage (houses damaged, and single or isolated groups of trees blown down); (**C**) F2 wind damage (houses unroofed or destroyed and extensive tree blowdowns) and F3 wind damage (houses blown down or destroyed, most trees down, and heavy automobiles lifted or overturned); (**D**) cumulative hurricane wind damage.

Panel A in Figure 9 shows the spatial extent of hurricane risk in which a total of 764 counties have experienced F0 wind damage (the loss of leaves and branches) over time, stretching from Southeast Texas to the far stretches of Maine. The counties within 100 miles of the coastline have been exposed to F0 wind strengths more than five times. Panel B reveals the areal extent of F1 damage (scattered blowdowns), and 455 counties have been exposed to F1-strength wind forces. As can be seen from Panel C, the areas exposed to F2 or F3 (extensive blowdowns) wind strengths are concentrated along the coastal regions of North Carolina, South Florida, and the Gulf of Mexico. As expected, F0- and F1-intensity winds traveled further inland compared to F2- and F3-scale winds that are more localized along the coastline (Panel D).

The areal extent of hurricane-driven storm surge is geographically concentrated along the coastal shoreline counties, whereas hurricane winds tend to affect the inland areas to a larger extent, penetrating deep into the inland areas of the United States. This is more apparent in northeastern states. A previous study showed that hurricanes that move north along the Atlantic Coast tend to have greater forward speed than hurricanes making landfall along the southern states due to the interaction of northern air masses, leading to greater inland penetration and, consequentially, higher damage impacts [68]. In comparison with the wind speed map defined by the American Society of Civil Engineers (ASCE) and the previous study by Logan and Xu [29] for the Gulf Coast region, this generalized damage boundary from storm surge and hurricane-force wind damage demonstrates similar findings, providing validation to the SLOSH and HURRECON modeling performed in this study.

3.2. At-Risk Populations in the Hurrican-Prone Coastal Counties

Based on the modeling of hurricane-related damage, this study defines "hurricane-prone coastal counties" as counties that are exposed to one form of hurricane damage, as shown in Figure 10. The modeled outputs of all hurricanes were aggregated into a singular geographic area to represent long-term historic cumulative damage over the past six decades. Combining the spatial extent of hurricane-damaged areas of F0, F1, F2, and F3 winds (Figure 10A) and storm surges (Figure 10B), the spatial coverage of this study area consists of 775 counties over 22 states (Figure 10C). The list of coastal counties defined in this study is set out in Appendix A. The areal extent defined in this study through hurricane modeling is similar to the coastal counties defined by Ache et al. [69] and Marsooli et al. [70], validating the result. However, the modeled output presents a more detailed profile of the affected counties, encompassing inland counties exposed to historical hurricane wind penetrations. This was used to describe the at-risk coastal populations susceptible to hurricane hazards in the United States.

The aggregated geographic extent of all hurricane-related damage shows a generalized and standardized pattern, with no seasonal or random variation across time and space [29]. The affected coastal counties in the Gulf Coast cover the majority of counties that are affected by hurricanes, up to approximately 200 miles from coastal shorelines. Meanwhile, the affected coastal counties of the Atlantic Coast are located up to 400 miles from the coast, reaching further inland than the Gulf Coast. The hurricane-prone coastal counties are geographically restricted to the Gulf of Mexico coastline and the eastern Atlantic Coast of the United States (i.e., the North Atlantic Basin region), excluding the Pacific Coast and the Great Lakes region, providing a baseline for describing the human settlement of the hurricane-impacted coastal shorelines [16,69,71].
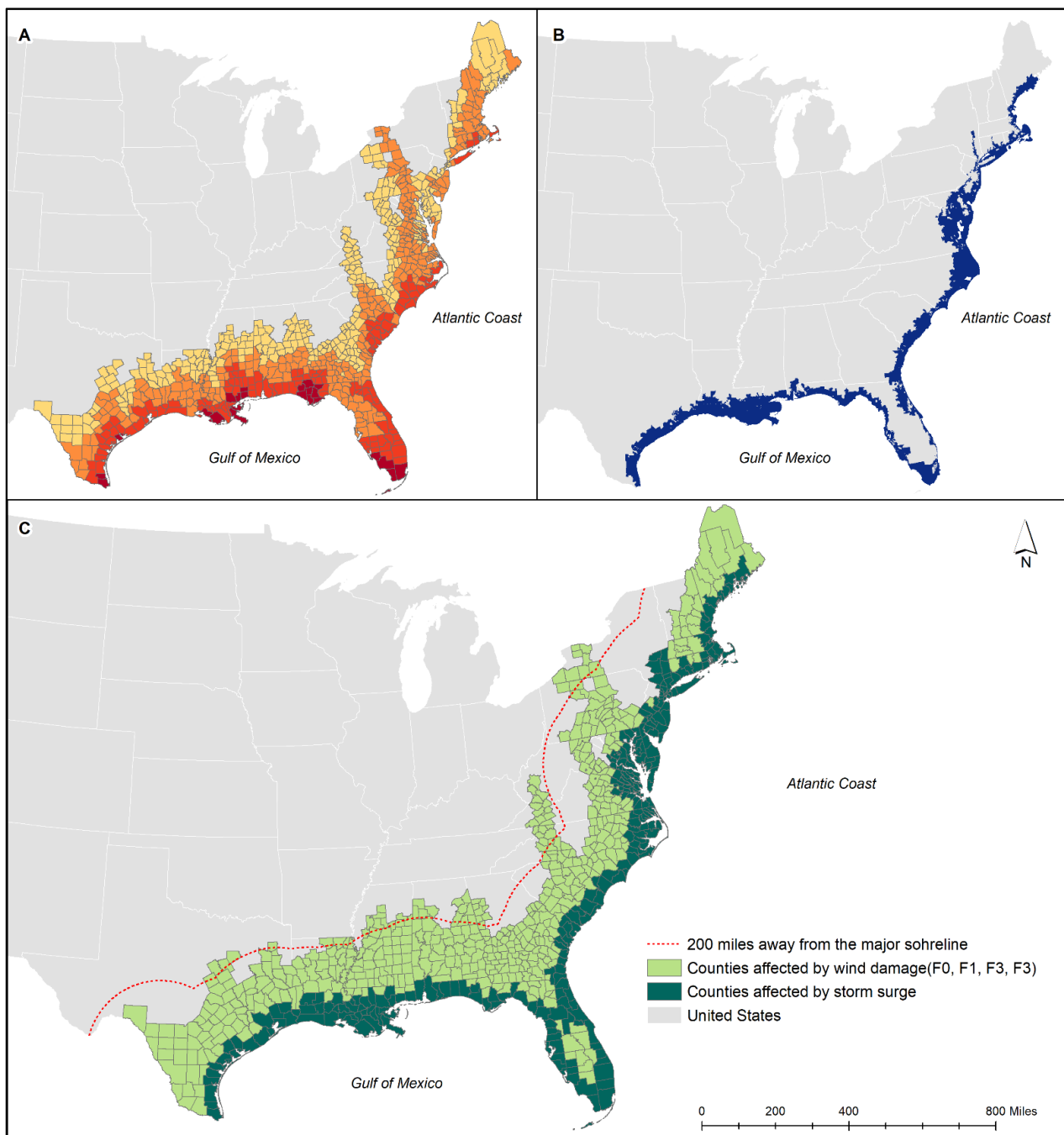
Figure 10. (**A**) The coastal counties affected by wind damage according to the Fujita scale (F0, F1, F2, and F3); (**B**) the coastal counties affected by storm surges; (**C**) the 775 hurricane-prone coastal counties defined in this study.

To supplement this analysis, this study further examined how many people have been living in residential areas in the U.S. hurricane coastal counties from 1970 to 2018 using the U.S. Decennial Census (1950, 1960) and the U.S. County Intercensal Datasets (1970–2018) in conjunction with the national land use/land cover data. To determine the number of people within each hurricane-affected zone, this study first calculated the percentage of developed/residential areas in each county/census tract that have been affected by wind damage and storm surges (i.e., damage fraction hereafter) by applying zonal analysis operations. The product of the damage fraction of storm surge and wind damage with the total population counts produced the number of at-risk populations exposed to cumulative hurricane damage over the decades. This filtered areal weighting

interpolation approach was adopted to disaggregate total populations to a target area—in this case, hurricane-affected zones—on the basis of the areal extent of storm surge damage and wind damage (measured by the Fujita scale—F0, F1, F2, and F3) [72–74].

The coastal counties are more overcrowded than the nation as a whole, and they are expected to grow in the future [16]. The total number of people living in coastal areas was 73 million in 1970, growing by a total of 100 million people between 1970 and 2000 (Figure 11). Although the population growth rate consistently declined after 2000, along with the national trend, there was a 63% increase in the coastal population from 1970 to 2018, exceeding 119 million in 2018. The population density of coastal counties is substantially greater than that of inland counties [16,75]. Coastal populations are facing multiple threats such as climate change and coastal hazards, exposing 36.5% of the U.S. total population to increasingly vulnerable situations (Figure 12). Along with rapid population growth and an economic construction boom, the coastal populations have been racially diversified, thereby further exacerbating their social vulnerability to hurricane hazards in the coastal counties over time [13,76].

Figure 13 presents how many people have been exposed to hurricane-related damage in absolute terms. It is apparent that the total population has continuously increased within each hurricane-affected area from 1950 to 2018. Wind damage is separated into different categories based on intensity (i.e., F0, F1, F2, and F3). While some of this growth might be due to the national trend, there is a higher exponential growth trend in F0 and F1 areas than the national trend. Approximately 165 million people are affected by some degree of wind damage during the study period.

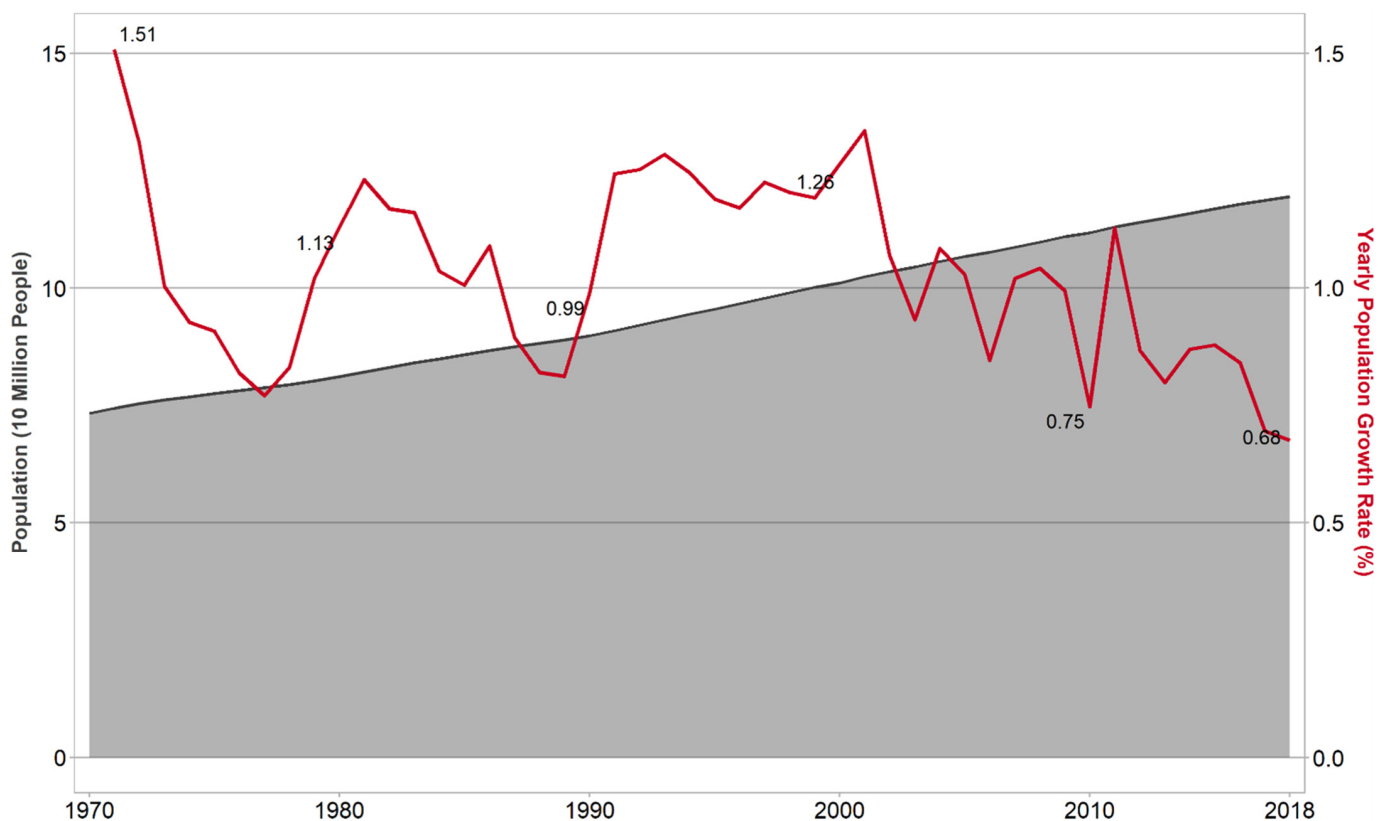**Figure 11.** The population trend of the coastal counties and growth rate (1970–2018).
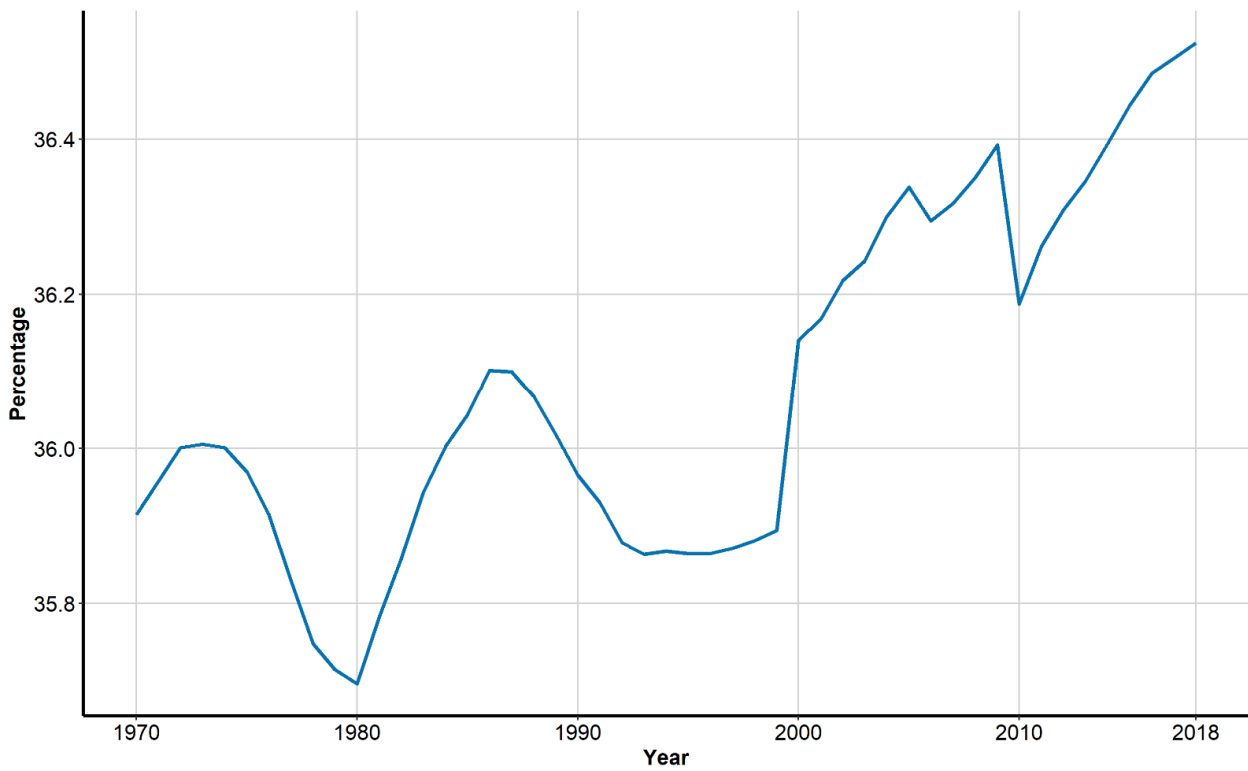
Figure 12. The percentage of the total U.S. population living in residential areas in the hurricane-prone coastal counties (1970–2018).
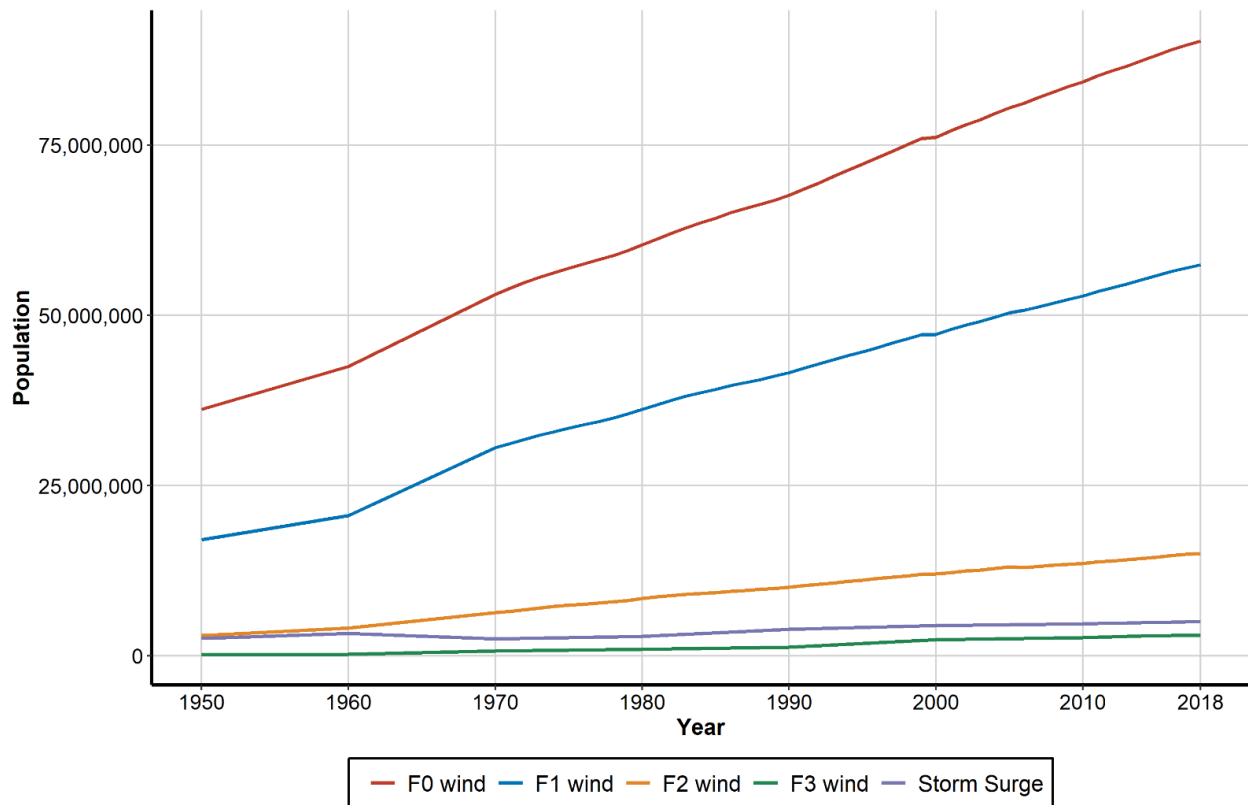

Figure 13. Total population exposed to hurricane-related damage in residential areas in the hurricane-prone coastal counties by different hurricane damage categories (1950–2018).

Generally, as hurricanes make landfall along the coast, wind speeds rapidly weaken due to the higher frictional effects of land surfaces and a lack of moisture and latent heat energy from the ocean [67]. However, tropical storms and hurricanes can travel hundreds of miles deep into interior counties after landfall, and the remnants of hurricanes may occasionally intensify or maintain their power for an extended period of time, possibly due to various physical processes and storm dynamics [77]. For instance, as seen from Hurricane Sandy, when a low-pressure storm system encounters the polar jet stream in the mid-latitudes, strong temperature gradients occur, and this may re-intensify its strength after making landfall. This process is known as "baroclinic enhancement". In addition, land surface characteristics (e.g., soil water content, vegetation types, land use, land cover) can play a major role in maintaining a tropical cyclone's intensity over land. Wet ground or soil with abundant moisture after precipitation events can be a latent source, providing enough heat energy to the storm (i.e., brown ocean effect) [78,79]. Therefore, the affected areas are not just limited to the immediate vicinity of coastal regions but also extend hundreds of miles from the immediate coastal shorelines (Figure 10).

In contrast, storm surge damage and F3 wind are highly localized along coastal areas, as shown in Figure 10. From the data in Figure 13, we can see that 5 million people resided in the residential areas that are affected by storm surge damage, and 3 million people resided in high-intensity wind (F3 scale) areas, as of 2018. To summarize, the overall demographic trends within hurricane-impacted areas reveal that the coastal populations are faster growing than the national average, and this growth puts more people at greater risk of hurricane hazards. This poses a challenge to policymakers as they need to understand a more complex population in order to make more informed decisions in mitigating coastal vulnerability to hurricane hazards.

4. Discussion

Hurricanes pose the greatest natural risk of damage to the United States' hurricane coasts and society [13]. Physical or locational vulnerability can be assessed based on the impacts, magnitude, and frequency of natural hazards, and geographical proximity to the source of natural hazards [22,29,80]. Hurricanes tend to occur at certain geographical locations, and the general patterns of occurrence are less likely to change in the future. Therefore, estimating and representing the cumulative hurricane patterns can offer a useful means to assess current and future hurricane risk. Due to the scarcity of data regarding historical hurricane-impacted areas, this study sought to determine the spatial extent and intensity of hurricane wind and storm surge damage of all hurricanes that made landfall along America's hurricane coasts from 1950 to 2018 [13]. Both the spatial extent and intensity of all hurricanes were estimated by utilizing geospatial big data datasets. The extensive results of the hurricane modeling were aggregated into a single surface, representing the longitudinal risk of hurricanes. As a result, 775 counties were found to comprise the hurricane at-risk zones that have experienced at least one instance of hurricane damage over the last six decades. Historical hurricanes that have affected the Gulf and Atlantic coastal areas revealed that storm surge damage in these areas extends up to approximately 41,000 km^2, and the largest extent of wind damage (F0) extends to approximately 1,300,000 km^2, in the conterminous United States.

This project is the first comprehensive investigation of hurricane vulnerability encompassing the Atlantic and Gulf Coasts stretching from Texas to Maine. The current study proposed the geographical extent of 775 hurricane-prone coastal counties that border the Gulf of Mexico and the eastern Atlantic Coast of the United States, excluding the Pacific Coast (Appendix A). By integrating the past and recent hurricane damage over long periods of time, the results delineate the zones at a high risk of hurricanes more accurately than arbitrarily defining the study areas. This delineation can be used as a tool in assessing coastal population vulnerability by federal agencies and researchers. For instance, the spatially explicit hurricane-prone regions can assist policymakers in developing targeted interventions for the national flood insurance program and coastal wind pool insurance.

The estimation of hurricane wind was based on the same parameters used in a previous empirical study that modeled historical hurricanes along the Gulf Coast [29]. Different parameters may result in more accurate estimations for storms that made landfall on the Atlantic Coast.

The population density of coastal counties is denser than the nation as a whole, and the populations in these counties are expected to grow in the future. Along with rapid population growth and an economic construction boom, the coastal populations have been racially diversified, thereby further exacerbating the potential social impact of hurricane hazards in the coastal counties [13,16,76]. Thus, based on the geographic extent of hurricane at-risk zones and land use data, this study performed zonal analysis to further examine how many coastal populations are exposed to the hurricane damage categories—storm surge damage and F0/F1/F2/F3 wind damage—within the residential areas. The findings from this study provide a fundamental basis for understanding the exposure of at-risk populations to hurricane-related damage within the coastal counties at a national scale. The resulting output of the hurricane-prone coastal counties also opens the potential to further examine the specific demographic characteristics of the at-risk populations, allowing for a further assessment of social vulnerability in these areas.

To provide a complete picture of place-based and population vulnerability within the hurricane at-risk areas, future studies should take into account more detailed demographic variables such as race/ethnicity, age groups, and income level. Exploring the demographic changes within the hurricane at-risk areas was purely descriptive; it was not possible to determine a causal relationship between long-term hurricane damage and population change. This study did not evaluate the hurricane-forced internal or intra-regional residential displacement, either temporarily or permanently, associated with post-disaster recovery processes and community resilience to these hurricane hazards. The spatial patterns of hurricane-induced residential mobility and its mechanism remain to be elucidated for further investigation. Future studies need to examine the links between the impacts of hurricane-related damage on local population change based on empirical statistical analysis and mixed method approaches more closely.

Appendix A. Hurricane-Prone Coastal Counties (n = 775) along the U.S. Atlantic and Gulf Coasts Defined in this Study

FIPS	Geography	FIPS	Geography
01001	Autauga County, Alabama	01123	Tallapoosa County, Alabama
01003	Baldwin County, Alabama	01125	Tuscaloosa County, Alabama
01005	Barbour County, Alabama	01127	Walker County, Alabama
01007	Bibb County, Alabama	01129	Washington County, Alabama
01011	Bullock County, Alabama	01131	Wilcox County, Alabama
01013	Butler County, Alabama	09001	Fairfield County, Connecticut
01015	Calhoun County, Alabama	09003	Hartford County, Connecticut
01017	Chambers County, Alabama	09005	Litchfield County, Connecticut
01019	Cherokee County, Alabama	09007	Middlesex County, Connecticut
01021	Chilton County, Alabama	09009	New Haven County, Connecticut
01023	Choctaw County, Alabama	09011	New London County, Connecticut
01025	Clarke County, Alabama	09013	Tolland County, Connecticut
01027	Clay County, Alabama	09015	Windham County, Connecticut
01029	Cleburne County, Alabama	10001	Kent County, Delaware
01031	Coffee County, Alabama	10003	New Castle County, Delaware
01035	Conecuh County, Alabama	10005	Sussex County, Delaware
01037	Coosa County, Alabama	11001	District of Columbia, District of Columbia
01039	Covington County, Alabama	12001	Alachua County, Florida
01041	Crenshaw County, Alabama	12003	Baker County, Florida
01045	Dale County, Alabama	12005	Bay County, Florida
01047	Dallas County, Alabama	12007	Bradford County, Florida
01051	Elmore County, Alabama	12009	Brevard County, Florida
01053	Escambia County, Alabama	12011	Broward County, Florida
01055	Etowah County, Alabama	12013	Calhoun County, Florida
01057	Fayette County, Alabama	12015	Charlotte County, Florida
01061	Geneva County, Alabama	12017	Citrus County, Florida
01063	Greene County, Alabama	12019	Clay County, Florida
01065	Hale County, Alabama	12021	Collier County, Florida
01067	Henry County, Alabama	12023	Columbia County, Florida
01069	Houston County, Alabama	12027	DeSoto County, Florida
01075	Lamar County, Alabama	12029	Dixie County, Florida
01081	Lee County, Alabama	12031	Duval County, Florida
01085	Lowndes County, Alabama	12033	Escambia County, Florida
01087	Macon County, Alabama	12035	Flagler County, Florida
01091	Marengo County, Alabama	12037	Franklin County, Florida
01093	Marion County, Alabama	12039	Gadsden County, Florida
01097	Mobile County, Alabama	12041	Gilchrist County, Florida
01099	Monroe County, Alabama	12043	Glades County, Florida
01101	Montgomery County, Alabama	12045	Gulf County, Florida
01105	Perry County, Alabama	12047	Hamilton County, Florida
01107	Pickens County, Alabama	12049	Hardee County, Florida
01109	Pike County, Alabama	12051	Hendry County, Florida
01111	Randolph County, Alabama	12053	Hernando County, Florida
01113	Russell County, Alabama	12055	Highlands County, Florida
01119	Sumter County, Alabama	12057	Hillsborough County, Florida
01121	Talladega County, Alabama	12059	Holmes County, Florida
12061	Indian River County, Florida	13031	Bulloch County, Georgia
12063	Jackson County, Florida	13033	Burke County, Georgia
12065	Jefferson County, Florida	13037	Calhoun County, Georgia
12067	Lafayette County, Florida	13039	Camden County, Georgia
12069	Lake County, Florida	13043	Candler County, Georgia
12071	Lee County, Florida	13045	Carroll County, Georgia
12073	Leon County, Florida	13049	Charlton County, Georgia

FIPS	Geography	FIPS	Geography
12075	Levy County, Florida	13051	Chatham County, Georgia
12077	Liberty County, Florida	13053	Chattahoochee County, Georgia
12079	Madison County, Florida	13061	Clay County, Georgia
12081	Manatee County, Florida	13065	Clinch County, Georgia
12083	Marion County, Florida	13069	Coffee County, Georgia
12085	Martin County, Florida	13071	Colquitt County, Georgia
12086	Miami-Dade County, Florida	13073	Columbia County, Georgia
12087	Monroe County, Florida	13075	Cook County, Georgia
12089	Nassau County, Florida	13077	Coweta County, Georgia
12091	Okaloosa County, Florida	13079	Crawford County, Georgia
12093	Okeechobee County, Florida	13081	Crisp County, Georgia
12095	Orange County, Florida	13087	Decatur County, Georgia
12097	Osceola County, Florida	13091	Dodge County, Georgia
12099	Palm Beach County, Florida	13093	Dooly County, Georgia
12101	Pasco County, Florida	13095	Dougherty County, Georgia
12103	Pinellas County, Florida	13097	Douglas County, Georgia
12105	Polk County, Florida	13099	Early County, Georgia
12107	Putnam County, Florida	13101	Echols County, Georgia
12109	St. Johns County, Florida	13103	Effingham County, Georgia
12111	St. Lucie County, Florida	13107	Emanuel County, Georgia
12115	Sarasota County, Florida	13109	Evans County, Georgia
12117	Seminole County, Florida	13125	Glascock County, Georgia
12119	Sumter County, Florida	13127	Glynn County, Georgia
12121	Suwannee County, Florida	13131	Grady County, Georgia
12123	Taylor County, Florida	13143	Haralson County, Georgia
12125	Union County, Florida	13145	Harris County, Georgia
12127	Volusia County, Florida	13149	Heard County, Georgia
12129	Wakulla County, Florida	13153	Houston County, Georgia
12131	Walton County, Florida	13155	Irwin County, Georgia
12133	Washington County, Florida	13161	Jeff Davis County, Georgia
13001	Appling County, Georgia	13163	Jefferson County, Georgia
13003	Atkinson County, Georgia	13165	Jenkins County, Georgia
13005	Bacon County, Georgia	13167	Johnson County, Georgia
13007	Baker County, Georgia	13173	Lanier County, Georgia
13017	Ben Hill County, Georgia	13175	Laurens County, Georgia
13019	Berrien County, Georgia	13177	Lee County, Georgia
13021	Bibb County, Georgia	13179	Liberty County, Georgia
13023	Bleckley County, Georgia	13183	Long County, Georgia
13025	Brantley County, Georgia	13185	Lowndes County, Georgia
13027	Brooks County, Georgia	13189	McDuffie County, Georgia
13029	Bryan County, Georgia	13191	McIntosh County, Georgia
13193	Macon County, Georgia	22023	Cameron Parish, Louisiana
13197	Marion County, Georgia	22025	Catahoula Parish, Louisiana
13201	Miller County, Georgia	22029	Concordia Parish, Louisiana
13205	Mitchell County, Georgia	22031	De Soto Parish, Louisiana
13209	Montgomery County, Georgia	22033	East Baton Rouge Parish, Louisiana
13215	Muscogee County, Georgia	22035	East Carroll Parish, Louisiana
13223	Paulding County, Georgia	22037	East Feliciana Parish, Louisiana
13225	Peach County, Georgia	22039	Evangeline Parish, Louisiana
13229	Pierce County, Georgia	22041	Franklin Parish, Louisiana
13233	Polk County, Georgia	22043	Grant Parish, Louisiana
13235	Pulaski County, Georgia	22045	Iberia Parish, Louisiana
13239	Quitman County, Georgia	22047	Iberville Parish, Louisiana
13243	Randolph County, Georgia	22049	Jackson Parish, Louisiana
13245	Richmond County, Georgia	22051	Jefferson Parish, Louisiana
13249	Schley County, Georgia	22053	Jefferson Davis Parish, Louisiana

FIPS	Geography	FIPS	Geography
13251	Screven County, Georgia	22055	Lafayette Parish, Louisiana
13253	Seminole County, Georgia	22057	Lafourche Parish, Louisiana
13259	Stewart County, Georgia	22059	La Salle Parish, Louisiana
13261	Sumter County, Georgia	22063	Livingston Parish, Louisiana
13267	Tattnall County, Georgia	22065	Madison Parish, Louisiana
13269	Taylor County, Georgia	22067	Morehouse Parish, Louisiana
13271	Telfair County, Georgia	22069	Natchitoches Parish, Louisiana
13273	Terrell County, Georgia	22071	Orleans Parish, Louisiana
13275	Thomas County, Georgia	22073	Ouachita Parish, Louisiana
13277	Tift County, Georgia	22075	Plaquemines Parish, Louisiana
13279	Toombs County, Georgia	22077	Pointe Coupee Parish, Louisiana
13283	Treutlen County, Georgia	22079	Rapides Parish, Louisiana
13285	Troup County, Georgia	22081	Red River Parish, Louisiana
13287	Turner County, Georgia	22083	Richland Parish, Louisiana
13289	Twiggs County, Georgia	22085	Sabine Parish, Louisiana
13299	Ware County, Georgia	22087	St. Bernard Parish, Louisiana
13301	Warren County, Georgia	22089	St. Charles Parish, Louisiana
13303	Washington County, Georgia	22091	St. Helena Parish, Louisiana
13305	Wayne County, Georgia	22093	St. James Parish, Louisiana
13307	Webster County, Georgia	22095	St. John the Baptist Parish, Louisiana
13309	Wheeler County, Georgia	22097	St. Landry Parish, Louisiana
13315	Wilcox County, Georgia	22099	St. Martin Parish, Louisiana
13319	Wilkinson County, Georgia	22101	St. Mary Parish, Louisiana
13321	Worth County, Georgia	22103	St. Tammany Parish, Louisiana
22001	Acadia Parish, Louisiana	22105	Tangipahoa Parish, Louisiana
22003	Allen Parish, Louisiana	22107	Tensas Parish, Louisiana
22005	Ascension Parish, Louisiana	22109	Terrebonne Parish, Louisiana
22007	Assumption Parish, Louisiana	22111	Union Parish, Louisiana
22009	Avoyelles Parish, Louisiana	22113	Vermilion Parish, Louisiana
22011	Beauregard Parish, Louisiana	22115	Vernon Parish, Louisiana
22013	Bienville Parish, Louisiana	22117	Washington Parish, Louisiana
22019	Calcasieu Parish, Louisiana	22121	West Baton Rouge Parish, Louisiana
22021	Caldwell Parish, Louisiana	22123	West Carroll Parish, Louisiana
22125	West Feliciana Parish, Louisiana	25017	Middlesex County, Massachusetts
22127	Winn Parish, Louisiana	25019	Nantucket County, Massachusetts
23001	Androscoggin County, Maine	25021	Norfolk County, Massachusetts
23003	Aroostook County, Maine	25023	Plymouth County, Massachusetts
23005	Cumberland County, Maine	25025	Suffolk County, Massachusetts
23007	Franklin County, Maine	25027	Worcester County, Massachusetts
23009	Hancock County, Maine	28001	Adams County, Mississippi
23011	Kennebec County, Maine	28005	Amite County, Mississippi
23013	Knox County, Maine	28007	Attala County, Mississippi
23015	Lincoln County, Maine	28015	Carroll County, Mississippi
23017	Oxford County, Maine	28019	Choctaw County, Mississippi
23019	Penobscot County, Maine	28021	Claiborne County, Mississippi
23021	Piscataquis County, Maine	28023	Clarke County, Mississippi
23023	Sagadahoc County, Maine	28025	Clay County, Mississippi
23025	Somerset County, Maine	28029	Copiah County, Mississippi
23027	Waldo County, Maine	28031	Covington County, Mississippi
23029	Washington County, Maine	28035	Forrest County, Mississippi
23031	York County, Maine	28037	Franklin County, Mississippi
24001	Allegany County, Maryland	28039	George County, Mississippi
24003	Anne Arundel County, Maryland	28041	Greene County, Mississippi
24005	Baltimore County, Maryland	28043	Grenada County, Mississippi
24009	Calvert County, Maryland	28045	Hancock County, Mississippi
24011	Caroline County, Maryland	28047	Harrison County, Mississippi
24013	Carroll County, Maryland	28049	Hinds County, Mississippi

FIPS	Geography	FIPS	Geography
24015	Cecil County, Maryland	28051	Holmes County, Mississippi
24017	Charles County, Maryland	28053	Humphreys County, Mississippi
24019	Dorchester County, Maryland	28059	Jackson County, Mississippi
24021	Frederick County, Maryland	28061	Jasper County, Mississippi
24023	Garrett County, Maryland	28063	Jefferson County, Mississippi
24025	Harford County, Maryland	28065	Jefferson Davis County, Mississippi
24027	Howard County, Maryland	28067	Jones County, Mississippi
24029	Kent County, Maryland	28069	Kemper County, Mississippi
24031	Montgomery County, Maryland	28073	Lamar County, Mississippi
24033	Prince George's County, Maryland	28075	Lauderdale County, Mississippi
24035	Queen Anne's County, Maryland	28077	Lawrence County, Mississippi
24037	St. Mary's County, Maryland	28079	Leake County, Mississippi
24039	Somerset County, Maryland	28083	Leflore County, Mississippi
24041	Talbot County, Maryland	28085	Lincoln County, Mississippi
24045	Wicomico County, Maryland	28087	Lowndes County, Mississippi
24047	Worcester County, Maryland	28089	Madison County, Mississippi
25001	Barnstable County, Massachusetts	28091	Marion County, Mississippi
25003	Berkshire County, Massachusetts	28097	Montgomery County, Mississippi
25005	Bristol County, Massachusetts	28099	Neshoba County, Mississippi
25007	Dukes County, Massachusetts	28101	Newton County, Mississippi
25009	Essex County, Massachusetts	28103	Noxubee County, Mississippi
25011	Franklin County, Massachusetts	28105	Oktibbeha County, Mississippi
25013	Hampden County, Massachusetts	28109	Pearl River County, Mississippi
25015	Hampshire County, Massachusetts	28111	Perry County, Mississippi
28113	Pike County, Mississippi	36039	Greene County, New York
28121	Rankin County, Mississippi	36047	Kings County, New York
28123	Scott County, Mississippi	36051	Livingston County, New York
28127	Simpson County, Mississippi	36055	Monroe County, New York
28129	Smith County, Mississippi	36059	Nassau County, New York
28131	Stone County, Mississippi	36061	New York County, New York
28147	Walthall County, Mississippi	36071	Orange County, New York
28149	Warren County, Mississippi	36073	Orleans County, New York
28153	Wayne County, Mississippi	36079	Putnam County, New York
28157	Wilkinson County, Mississippi	36081	Queens County, New York
28159	Winston County, Mississippi	36085	Richmond County, New York
28161	Yalobusha County, Mississippi	36087	Rockland County, New York
28163	Yazoo County, Mississippi	36101	Steuben County, New York
33001	Belknap County, New Hampshire	36103	Suffolk County, New York
33003	Carroll County, New Hampshire	36111	Ulster County, New York
33005	Cheshire County, New Hampshire	36119	Westchester County, New York
33007	Coos County, New Hampshire	37003	Alexander County, North Carolina
33009	Grafton County, New Hampshire	37005	Alleghany County, North Carolina
33011	Hillsborough County, New Hampshire	37007	Anson County, North Carolina
33013	Merrimack County, New Hampshire	37009	Ashe County, North Carolina
33015	Rockingham County, New Hampshire	37013	Beaufort County, North Carolina
33017	Strafford County, New Hampshire	37015	Bertie County, North Carolina
33019	Sullivan County, New Hampshire	37017	Bladen County, North Carolina
34001	Atlantic County, New Jersey	37019	Brunswick County, North Carolina
34003	Bergen County, New Jersey	37023	Burke County, North Carolina
34005	Burlington County, New Jersey	37025	Cabarrus County, North Carolina
34007	Camden County, New Jersey	37027	Caldwell County, North Carolina
34009	Cape May County, New Jersey	37029	Camden County, North Carolina
34011	Cumberland County, New Jersey	37031	Carteret County, North Carolina
34013	Essex County, New Jersey	37035	Catawba County, North Carolina
34015	Gloucester County, New Jersey	37037	Chatham County, North Carolina
34017	Hudson County, New Jersey	37041	Chowan County, North Carolina

FIPS	Geography	FIPS	Geography
34019	Hunterdon County, New Jersey	37045	Cleveland County, North Carolina
34021	Mercer County, New Jersey	37047	Columbus County, North Carolina
34023	Middlesex County, New Jersey	37049	Craven County, North Carolina
34025	Monmouth County, New Jersey	37051	Cumberland County, North Carolina
34029	Ocean County, New Jersey	37053	Currituck County, North Carolina
34031	Passaic County, New Jersey	37055	Dare County, North Carolina
34033	Salem County, New Jersey	37061	Duplin County, North Carolina
34035	Somerset County, New Jersey	37063	Durham County, North Carolina
34039	Union County, New Jersey	37065	Edgecombe County, North Carolina
36003	Allegany County, New York	37069	Franklin County, North Carolina
36005	Bronx County, New York	37071	Gaston County, North Carolina
36009	Cattaraugus County, New York	37073	Gates County, North Carolina
36013	Chautauqua County, New York	37077	Granville County, North Carolina
36021	Columbia County, New York	37079	Greene County, North Carolina
36027	Dutchess County, New York	37083	Halifax County, North Carolina
36037	Genesee County, New York	37085	Harnett County, North Carolina
37091	Hertford County, North Carolina	42035	Clinton County, Pennsylvania
37093	Hoke County, North Carolina	42041	Cumberland County, Pennsylvania
37095	Hyde County, North Carolina	42043	Dauphin County, Pennsylvania
37097	Iredell County, North Carolina	42045	Delaware County, Pennsylvania
37101	Johnston County, North Carolina	42047	Elk County, Pennsylvania
37103	Jones County, North Carolina	42051	Fayette County, Pennsylvania
37105	Lee County, North Carolina	42055	Franklin County, Pennsylvania
37107	Lenoir County, North Carolina	42057	Fulton County, Pennsylvania
37109	Lincoln County, North Carolina	42061	Huntingdon County, Pennsylvania
37117	Martin County, North Carolina	42067	Juniata County, Pennsylvania
37119	Mecklenburg County, North Carolina	42071	Lancaster County, Pennsylvania
37125	Moore County, North Carolina	42075	Lebanon County, Pennsylvania
37127	Nash County, North Carolina	42081	Lycoming County, Pennsylvania
37129	New Hanover County, North Carolina	42083	McKean County, Pennsylvania
37131	Northampton County, North Carolina	42087	Mifflin County, Pennsylvania
37133	Onslow County, North Carolina	42091	Montgomery County, Pennsylvania
37135	Orange County, North Carolina	42097	Northumberland County, Pennsylvania
37137	Pamlico County, North Carolina	42099	Perry County, Pennsylvania
37139	Pasquotank County, North Carolina	42101	Philadelphia County, Pennsylvania
37141	Pender County, North Carolina	42109	Snyder County, Pennsylvania
37143	Perquimans County, North Carolina	42111	Somerset County, Pennsylvania
37145	Person County, North Carolina	42117	Tioga County, Pennsylvania
37147	Pitt County, North Carolina	42119	Union County, Pennsylvania
37153	Richmond County, North Carolina	42123	Warren County, Pennsylvania
37155	Robeson County, North Carolina	42133	York County, Pennsylvania
37159	Rowan County, North Carolina	44001	Bristol County, Rhode Island
37163	Sampson County, North Carolina	44003	Kent County, Rhode Island
37165	Scotland County, North Carolina	44005	Newport County, Rhode Island
37167	Stanly County, North Carolina	44007	Providence County, Rhode Island
37177	Tyrrell County, North Carolina	44009	Washington County, Rhode Island
37179	Union County, North Carolina	45003	Aiken County, South Carolina
37181	Vance County, North Carolina	45005	Allendale County, South Carolina
37183	Wake County, North Carolina	45009	Bamberg County, South Carolina
37185	Warren County, North Carolina	45011	Barnwell County, South Carolina
37187	Washington County, North Carolina	45013	Beaufort County, South Carolina
37189	Watauga County, North Carolina	45015	Berkeley County, South Carolina
37191	Wayne County, North Carolina	45017	Calhoun County, South Carolina
37193	Wilkes County, North Carolina	45019	Charleston County, South Carolina
37195	Wilson County, North Carolina	45021	Cherokee County, South Carolina
42001	Adams County, Pennsylvania	45023	Chester County, South Carolina

FIPS	Geography	FIPS	Geography
42009	Bedford County, Pennsylvania	45025	Chesterfield County, South Carolina
42011	Berks County, Pennsylvania	45027	Clarendon County, South Carolina
42013	Blair County, Pennsylvania	45029	Colleton County, South Carolina
42017	Bucks County, Pennsylvania	45031	Darlington County, South Carolina
42021	Cambria County, Pennsylvania	45033	Dillon County, South Carolina
42023	Cameron County, Pennsylvania	45035	Dorchester County, South Carolina
42027	Centre County, Pennsylvania	45037	Edgefield County, South Carolina
42029	Chester County, Pennsylvania	45039	Fairfield County, South Carolina
45041	Florence County, South Carolina	48163	Frio County, Texas
45043	Georgetown County, South Carolina	48167	Galveston County, Texas
45049	Hampton County, South Carolina	48175	Goliad County, Texas
45051	Horry County, South Carolina	48177	Gonzales County, Texas
45053	Jasper County, South Carolina	48183	Gregg County, Texas
45055	Kershaw County, South Carolina	48185	Grimes County, Texas
45057	Lancaster County, South Carolina	48187	Guadalupe County, Texas
45061	Lee County, South Carolina	48199	Hardin County, Texas
45063	Lexington County, South Carolina	48201	Harris County, Texas
45067	Marion County, South Carolina	48209	Hays County, Texas
45069	Marlboro County, South Carolina	48215	Hidalgo County, Texas
45071	Newberry County, South Carolina	48217	Hill County, Texas
45075	Orangeburg County, South Carolina	48225	Houston County, Texas
45079	Richland County, South Carolina	48239	Jackson County, Texas
45081	Saluda County, South Carolina	48241	Jasper County, Texas
45085	Sumter County, South Carolina	48245	Jefferson County, Texas
45089	Williamsburg County, South Carolina	48247	Jim Hogg County, Texas
45091	York County, South Carolina	48249	Jim Wells County, Texas
47091	Johnson County, Tennessee	48255	Karnes County, Texas
48001	Anderson County, Texas	48261	Kenedy County, Texas
48005	Angelina County, Texas	48271	Kinney County, Texas
48007	Aransas County, Texas	48273	Kleberg County, Texas
48013	Atascosa County, Texas	48283	La Salle County, Texas
48015	Austin County, Texas	48285	Lavaca County, Texas
48021	Bastrop County, Texas	48287	Lee County, Texas
48025	Bee County, Texas	48289	Leon County, Texas
48027	Bell County, Texas	48291	Liberty County, Texas
48029	Bexar County, Texas	48297	Live Oak County, Texas
48035	Bosque County, Texas	48309	McLennan County, Texas
48039	Brazoria County, Texas	48311	McMullen County, Texas
48041	Brazos County, Texas	48313	Madison County, Texas
48047	Brooks County, Texas	48321	Matagorda County, Texas
48051	Burleson County, Texas	48323	Maverick County, Texas
48055	Caldwell County, Texas	48325	Medina County, Texas
48057	Calhoun County, Texas	48331	Milam County, Texas
48061	Cameron County, Texas	48339	Montgomery County, Texas
48071	Chambers County, Texas	48347	Nacogdoches County, Texas
48073	Cherokee County, Texas	48351	Newton County, Texas
48089	Colorado County, Texas	48355	Nueces County, Texas
48091	Comal County, Texas	48361	Orange County, Texas
48099	Coryell County, Texas	48373	Polk County, Texas
48123	DeWitt County, Texas	48391	Refugio County, Texas
48127	Dimmit County, Texas	48395	Robertson County, Texas
48131	Duval County, Texas	48401	Rusk County, Texas
48139	Ellis County, Texas	48403	Sabine County, Texas
48145	Falls County, Texas	48405	San Augustine County, Texas
48149	Fayette County, Texas	48407	San Jacinto County, Texas
48157	Fort Bend County, Texas	48409	San Patricio County, Texas

FIPS	Geography	FIPS	Geography
48419	Shelby County, Texas	51093	Isle of Wight County, Virginia
48423	Smith County, Texas	51095	James City County, Virginia
48427	Starr County, Texas	51097	King and Queen County, Virginia
48453	Travis County, Texas	51099	King George County, Virginia
48455	Trinity County, Texas	51101	King William County, Virginia
48457	Tyler County, Texas	51103	Lancaster County, Virginia
48459	Upshur County, Texas	51107	Loudoun County, Virginia
48463	Uvalde County, Texas	51109	Louisa County, Virginia
48465	Val Verde County, Texas	51111	Lunenburg County, Virginia
48469	Victoria County, Texas	51113	Madison County, Virginia
48471	Walker County, Texas	51115	Mathews County, Virginia
48473	Waller County, Texas	51117	Mecklenburg County, Virginia
48477	Washington County, Texas	51119	Middlesex County, Virginia
48479	Webb County, Texas	51125	Nelson County, Virginia
48481	Wharton County, Texas	51127	New Kent County, Virginia
48489	Willacy County, Texas	51131	Northampton County, Virginia
48491	Williamson County, Texas	51133	Northumberland County, Virginia
48493	Wilson County, Texas	51135	Nottoway County, Virginia
48505	Zapata County, Texas	51137	Orange County, Virginia
48507	Zavala County, Texas	51139	Page County, Virginia
50025	Windham County, Vermont	51145	Powhatan County, Virginia
50027	Windsor County, Vermont	51147	Prince Edward County, Virginia
51001	Accomack County, Virginia	51149	Prince George County, Virginia
51003	Albemarle County, Virginia	51153	Manassas city, Virginia
51007	Amelia County, Virginia	51153	Manassas Park city, Virginia
51011	Appomattox County, Virginia	51153	Prince William County, Virginia
51013	Arlington County, Virginia	51157	Rappahannock County, Virginia
51021	Bland County, Virginia	51159	Richmond County, Virginia
51025	Brunswick County, Virginia	51165	Rockingham County, Virginia
51029	Buckingham County, Virginia	51171	Shenandoah County, Virginia
51033	Caroline County, Virginia	51173	Smyth County, Virginia
51036	Charles City County, Virginia	51175	Southampton County, Virginia
51037	Charlotte County, Virginia	51177	Spotsylvania County, Virginia
51041	Chesterfield County, Virginia	51179	Stafford County, Virginia
51047	Culpeper County, Virginia	51181	Surry County, Virginia
51049	Cumberland County, Virginia	51183	Sussex County, Virginia
51053	Dinwiddie County, Virginia	51185	Tazewell County, Virginia
51057	Essex County, Virginia	51191	Washington County, Virginia
51059	Fairfax County, Virginia	51193	Westmoreland County, Virginia
51065	Fluvanna County, Virginia	51197	Wythe County, Virginia
51073	Gloucester County, Virginia	51199	York County, Virginia
51075	Goochland County, Virginia	51550	Chesapeake city, Virginia
51077	Grayson County, Virginia	51650	Hampton city, Virginia
51079	Greene County, Virginia	51683	Manassas city, Virginia
51081	Greensville County, Virginia	51685	Manassas Park city, Virginia
51083	Halifax County, Virginia	51700	Newport News city, Virginia
51085	Hanover County, Virginia	51730	Petersburg city, Virginia
51087	Henrico County, Virginia	51760	Richmond city, Virginia
51800	Suffolk city, Virginia	54039	Kanawha County, West Virginia
51810	Virginia Beach city, Virginia	54047	McDowell County, West Virginia
54005	Boone County, West Virginia	54055	Mercer County, West Virginia
54023	Grant County, West Virginia	54057	Mineral County, West Virginia
54027	Hampshire County, West Virginia	54081	Raleigh County, West Virginia
54031	Hardy County, West Virginia	54109	Wyoming County, West Virginia

References

1. Arkema, K.K.; Guannel, G.; Verutes, G.; Wood, S.A.; Guerry, A.; Ruckelshaus, M.; Kareiva, P.; Lacayo, M.; Silver, J.M. Coastal habitats shield people and property from sea-level rise and storms. *Nat. Clim. Chang.* **2013**, *3*, 913–918. [CrossRef]
2. Changnon, S.A.; Pielke, R.A., Jr.; Changnon, D.; Sylves, R.T.; Pulwarty, R. Human factors explain the increased losses from weather and climate extremes. *Bull. Am. Meteorol. Soc.* **2000**, *81*, 437–442. [CrossRef]
3. Emanuel, K. Global warming effects on US hurricane damage. *Weather Clim. Soc.* **2011**, *3*, 261–268. [CrossRef]
4. National Academies of Sciences, Engineering and Medicine. *Attribution of Extreme Weather Events in the Context of Climate Change*; National Academies Press: Washington, DC, USA, 2016.
5. Rahmstorf, S. Rising hazard of storm-surge flooding. *Proc. Natl. Acad. Sci. USA* **2017**, *114*, 11806–11808. [CrossRef]
6. Diaz, H.F.; Pulwarty, R.S. *Hurricanes: Climate and Socioeconomic Impacts*; Springer: Berlin/Heidelberg, Germany, 2012.
7. NOAA Office for Coastal Management. Fast Facts—Hurricane Coasts. Available online: https://coast.noaa.gov/states/fast-facts/hurricane-costs.html (accessed on 16 September 2021).
8. Weinkle, J.; Landsea, C.; Collins, D.; Musulin, R.; Crompton, R.P.; Klotzbach, P.J.; Pielke, R. Normalized hurricane damage in the continental United States 1900–2017. *Nat. Sustain.* **2018**, *1*, 808–813. [CrossRef]
9. Dolan, R.; Davis, R.E. Coastal storm hazards. *J. Coast. Res.* **1994**, 103–114.
10. Glahn, B.; Taylor, A.; Kurkowski, N.; Shaffer, W.A. The role of the SLOSH model in National Weather Service storm surge forecasting. *Natl. Weather Dig.* **2009**, *33*, 3–14.
11. Lin, N.; Emanuel, K.A.; Smith, J.A.; Vanmarcke, E. Risk assessment of hurricane storm surge for New York City. *J. Geophys. Res. Atmos.* **2010**, *115*. [CrossRef]
12. Lin, N.; Emanuel, K.; Oppenheimer, M.; Vanmarcke, E. Physically based assessment of hurricane surge threat under climate change. *Nat. Clim. Chang.* **2012**, *2*, 462–467. [CrossRef]
13. Cutter, S.L.; Johnson, L.A.; Finch, C.; Berry, M. The US hurricane coasts: Increasingly vulnerable? *Environ. Sci. Policy Sustain. Dev.* **2007**, *49*, 8–21. [CrossRef]
14. Lam, N.-N.; Arenas, H.; Li, Z.; Liu, K.-B. An estimate of population impacted by climate change along the US coast. *J. Coast. Res.* **2009**, 1522–1526. Available online: https://www.jstor.org/stable/25738044 (accessed on 1 September 2021).
15. Donner, W.; Rodríguez, H. Population composition, migration and inequality: The influence of demographic changes on disaster risk and vulnerability. *Soc. Forces* **2008**, *87*, 1089–1114. [CrossRef]
16. Crossett, K.A.; Brent; Pacheco, P.; Haber, K. *National Coastal Population Report: Population Trends from 1970 to 2020*; NOAA Office for Coastal Management: Silver Spring, MD, USA, 2013.
17. Maul, G.A.; Duedall, I.W. Demography of Coastal Populations. In *Encyclopedia of Coastal Science*; Finkl, C.W., Makowski, C., Eds.; Springer: Cham, Switzerland, 2019; pp. 692–700.
18. Cohen, D.T. About 60.2M Live in Areas Most Vulnerable to Hurricanes. Available online: https://www.census.gov/library/stories/2019/07/millions-of-americans-live-coastline-regions.html (accessed on 16 September 2021).
19. Pielke, R.A. Vulnerability to hurricanes along the US Atlantic and Gulf coasts: Considerations of the use of long-term forecasts. In *Hurricanes*; Springer: Berlin/Heidelberg, Germany, 1997; pp. 147–184.
20. Pompe, J.; Haluska, J. Estimating the Vulnerability of US Coastal Areas to Hurricane Damage. In *Recent Hurricane Research-Climate, Dynamics and Societal Impacts*; Lupo, A., Ed.; IntechOpen: London, UK, 2011; pp. 407–418.
21. Smith, K. *Environmental Hazards: Assessing Risk and Reducing Disaster*, 6th ed.; Routledge: New York, NY, USA, 2013.
22. Cutter, S.L. *American Hazardscapes: The Regionalization of Hazards and Disasters*; Joseph Henry Press: Washington, DC, USA, 2001.
23. Forbes, C.; Rhome, J.; Mattocks, C.; Taylor, A. Predicting the storm surge threat of Hurricane Sandy with the National Weather Service SLOSH model. *J. Mar. Sci. Eng.* **2014**, *2*, 437–476. [CrossRef]
24. Dietrich, J.; Dawson, C.; Proft, J.; Howard, M.; Wells, G.; Fleming, J.; Luettich, R.; Westerink, J.; Cobell, Z.; Vitse, M. Real-time forecasting and visualization of hurricane waves and storm surge using SWAN+ ADCIRC and FigureGen. In *Computational Challenges in the Geosciences*; Springer: Berlin/Heidelberg, Germany, 2013; pp. 49–70.
25. Dietrich, J.; Zijlema, M.; Westerink, J.; Holthuijsen, L.; Dawson, C.; Luettich, R., Jr.; Jensen, R.; Smith, J.; Stelling, G.; Stone, G. Modeling hurricane waves and storm surge using integrally-coupled, scalable computations. *Coast. Eng.* **2011**, *58*, 45–65. [CrossRef]
26. Powell, M.D.; Murillo, S.; Dodge, P.; Uhlhorn, E.; Gamache, J.; Cardone, V.; Cox, A.; Otero, S.; Carrasco, N.; Annane, B. Reconstruction of Hurricane Katrina's wind fields for storm surge and wave hindcasting. *Ocean Eng.* **2010**, *37*, 26–36. [CrossRef]
27. Anderson, G.; Schumacher, A.; Guikema, S.; Quiring, S.; Ferreri, J.; Staid, A.; Guo, M.; Ming, L.; Zhu, L. Stormwindmodel: Model Tropical Cyclone Wind Speeds.(R Package Version 0.1.4) 2020. Available online: http://cran.nexr.com/web/packages/stormwindmodel/index.html (accessed on 1 October 2021).
28. Anderson, G.B.; Ferreri, J.; Al-Hamdan, M.; Crosson, W.; Schumacher, A.; Guikema, S.; Quiring, S.; Eddelbuettel, D.; Yan, M.; Peng, R.D. Assessing United States county-level exposure for research on tropical cyclones and human health. *Environ. Health Perspect.* **2020**, *128*, 107009. [CrossRef]
29. Logan, J.R.; Xu, Z. Vulnerability to hurricane damage on the US Gulf Coast since 1950. *Geogr. Rev.* **2015**, *105*, 133–155. [CrossRef]
30. Füssel, H.-M. Vulnerability: A generally applicable conceptual framework for climate change research. *Glob. Environ. Chang.* **2007**, *17*, 155–167. [CrossRef]
31. Cutter, S.L. The vulnerability of science and the science of vulnerability. *Ann. Assoc. Am. Geogr.* **2003**, *93*, 1–12. [CrossRef]

32. Cutter, S.L. Social science perspectives on hazards and vulnerability science. In *Geophysical Hazards: Minimizing Risk, Maximizing Awareness*; Beer, T., Ed.; Springer: Dordrecht, The Netherlands, 2009; pp. 17–30.
33. Chi, H.; Pitter, S.; Li, N.; Tian, H. Big data solutions to interpreting complex systems in the environment. In *Guide to Big Data Applications*; Springer: Berlin/Heidelberg, Germany, 2018; pp. 107–124.
34. Abarca-Alvarez, F.J.; Reinoso-Bellido, R.; Campos-Sánchez, F.S. Decision model for predicting social vulnerability using artificial intelligence. *ISPRS Int. J. Geo-Inf.* **2019**, *8*, 575. [CrossRef]
35. Martín, Y.; Li, Z.; Cutter, S.L. Leveraging Twitter to gauge evacuation compliance: Spatiotemporal analysis of Hurricane Matthew. *PLoS ONE* **2017**, *12*, e0181701. [CrossRef]
36. Yang, C.; Clarke, K.; Shekhar, S.; Tao, C.V. Big Spatiotemporal Data Analytics: A research and innovation frontier. *Int. J. Geogr. Inf. Sci.* **2020**, 1075–1088. [CrossRef]
37. Yu, M.; Yang, C.; Li, Y. Big data in natural disaster management: A review. *Geosciences* **2018**, *8*, 165. [CrossRef]
38. Hashem, I.A.T.; Yaqoob, I.; Anuar, N.B.; Mokhtar, S.; Gani, A.; Khan, S.U. The rise of "big data" on cloud computing: Review and open research issues. *Inf. Syst.* **2015**, *47*, 98–115. [CrossRef]
39. Miller, H.J.; Goodchild, M.F. Data-driven geography. *GeoJournal* **2015**, *80*, 449–461. [CrossRef]
40. Reynard, D. Five classes of geospatial data and the barriers to using them. *Geogr. Compass* **2018**, *12*, e12364. [CrossRef]
41. Jarvinen, B.R.; Neumann, C.J.; Davis, M.A. *A Tropical Cyclone Data Tape for the North Atlantic Basin, 1886–1983: Contents, Limitations, and Uses*; National Hurricane Center: Miami, FL, USA, 1984.
42. Landsea, C.W.; Franklin, J.L. Atlantic hurricane database uncertainty and presentation of a new database format. *Mon. Weather Rev.* **2013**, *141*, 3576–3592. [CrossRef]
43. Landsea, C.W.; Franklin, J.L.; Beven, J.L. *The revised Atlantic hurricane database (HURDAT2)*; National Hurricane Center: Miami, FL, USA, 2015.
44. Allen, T.R.; Sanchagrin, S.; McLeod, G. Geovisualization for storm surge risk communication. In Proceedings of the Special Joint Symposium of ISPRS Technical Commission IV & AutoCaro in Conjunction with ASPRS/CaGIS 2010 Fall Specialty Conference, Orlando, FL, USA, 15–19 November 2010; pp. 15–19.
45. Zachry, B.C.; Booth, W.J.; Rhome, J.R.; Sharon, T.M. A national view of storm surge risk and inundation. *Weather Clim. Soc.* **2015**, *7*, 109–117. [CrossRef]
46. Jelesnianski, C.P.; Chen, J.; Shaffer, W.A. *SLOSH: Sea, Lake, and Overland Surges from Hurricanes*; NOAA Technical Report NWS 48; National Oceanic and Atmospheric Administration, U.S. Department of Commerce: Silver Spring, MD, USA, 1992.
47. Luther, M.E.; Merz, C.R.; Scudder, J.; Baig, S.R.; Pralgo, J.L.; Thompson, D.; Gill, S.; Hovis, G. Water level observations for storm surge. *Mar. Technol. Soc. J.* **2007**, *41*, 35–43. [CrossRef]
48. Yang, K.; Paramygin, V.A.; Sheng, Y.P. A rapid forecasting and mapping system of storm surge and coastal flooding. *Weather Forecast.* **2020**, *35*, 1663–1681. [CrossRef]
49. Conver, A.; Sepanik, J.; Louangsaysongkham, B.; Miller, S. *Sea, Lake, and Overland Surges from Hurricanes (SLOSH) Basin Development Handbook v2.0*; NOAA/NWS/Meteorological Development Laboratory: Silver Springs, MD, USA, 2008.
50. Allen, T.R.; Sanchagrin, S.; McLeod, G. Visualization for hurricane storm surge risk awareness and emergency communication. In *Approaches to Disaster Management—Examining the Implications of Hazards, Emergencies and Disasters*; Tiefenbacher, J.P., Ed.; IntechOpen: London, UK, 2013.
51. Mayo, T.; Lin, N.J.A. The effect of the surface wind field representation in the operational storm surge model of the National Hurricane Center. *Atmosphere* **2019**, *10*, 193. [CrossRef]
52. Mercado, A. On the use of NOAA''s storm surge model, SLOSH, in managing coastal hazards—The experience in Puerto Rico. *Nat. Hazards* **1994**, *10*, 235–246. [CrossRef]
53. Frazier, T.G.; Wood, N.; Yarnal, B.; Bauer, D.H. Influence of potential sea level rise on societal vulnerability to hurricane storm-surge hazards, Sarasota County, Florida. *Appl. Geogr.* **2010**, *30*, 490–505. [CrossRef]
54. Houston, S.H.; Shaffer, W.A.; Powell, M.D.; Chen, J. Comparisons of HRD and SLOSH surface wind fields in hurricanes: Implications for storm surge modeling. *Weather Forecast.* **1999**, *14*, 671–686. [CrossRef]
55. Maloney, M.C.; Preston, B.L. A geospatial dataset for US hurricane storm surge and sea-level rise vulnerability: Development and case study applications. *Clim. Risk Manag.* **2014**, *2*, 26–41. [CrossRef]
56. Boose, E.R.; Chamberlin, K.E.; Foster, D.R. Landscape and regional impacts of hurricanes in New England. *Ecol. Monogr.* **2001**, *71*, 27–48. [CrossRef]
57. Boose, E.R.; Serrano, M.I.; Foster, D.R. Landscape and regional impacts of hurricanes in Puerto Rico. *Ecol. Monogr.* **2004**, *74*, 335–352. [CrossRef]
58. Busby, P.E.; Canham, C.D.; Motzkin, G.; Foster, D.R. Forest response to chronic hurricane disturbance in coastal New England. *J. Veg. Sci.* **2009**, *20*, 487–497. [CrossRef]
59. Batke, S.P.; Jocque, M.; Kelly, D.L. Modelling hurricane exposure and wind speed on a mesoclimate scale: A case study from Cusuco NP, Honduras. *PLoS ONE* **2014**, *9*, e91306. [CrossRef]
60. Boose, E.R.; Foster, D.R.; Fluet, M. Hurricane impacts to tropical and temperate forest landscapes. *Ecol. Monogr.* **1994**, *64*, 369–400. [CrossRef]
61. Fujita, T.T. *Proposed Characterization of Tornadoes and Hurricanes by Area and Intensity*; University of Chicago: Chicago, IL, USA, 1971.

62. Womble, J.A.; Smith, D.A.; Mehta, K.C.; McDonald, J.R. The enhanced Fujita Scale: For use beyond tornadoes? In Proceedings of the Fifth Forensic Engineering: Pathology of the Built Environment, Washington, DC, USA, 11–14 November 2009; pp. 699–708.
63. Potter, S. Fine-Tuning Fujita: After 35 years, a new scale for rating tornadoes takes effect. *Weatherwise* **2007**, *60*, 64–71. [CrossRef]
64. Doswell III, C.A.; Brooks, H.E.; Dotzek, N. On the implementation of the enhanced Fujita scale in the USA. *Atmos. Res.* **2009**, *93*, 554–563. [CrossRef]
65. Boon, J.D. Evidence of sea level acceleration at US and Canadian tide stations, Atlantic Coast, North America. *J. Coast. Res.* **2012**, *28*, 1437–1445. [CrossRef]
66. Sallenger, A.H.; Doran, K.S.; Howd, P.A. Hotspot of accelerated sea-level rise on the Atlantic coast of North America. *Nat. Clim. Chang.* **2012**, *2*, 884–888. [CrossRef]
67. Smith, R.K.; Montgomery, M.T. Understanding hurricanes. *Weather* **2016**, *71*, 219–223. [CrossRef]
68. Coch, N.K. Hurricane hazards along the northeastern Atlantic coast of the United States. *J. Coast. Res.* **1994**, *12*, 115–147.
69. Ache, B.W.; Crossett, K.M.; Pacheco, P.A.; Adkins, J.E.; Wiley, P.C. "The coast" is complicated: A model to consistently describe the nation's coastal population. *Estuaries Coasts* **2015**, *38*, 151–155. [CrossRef]
70. Marsooli, R.; Lin, N.; Emanuel, K.; Feng, K. Climate change exacerbates hurricane flood hazards along US Atlantic and Gulf Coasts in spatially varying patterns. *Nat. Commun.* **2019**, *10*, 3785. [CrossRef]
71. Strobl, E. The economic growth impact of hurricanes: Evidence from US coastal counties. *Rev. Econ. Stat.* **2011**, *93*, 575–589. [CrossRef]
72. Maantay, J.A.; Maroko, A.R.; Herrmann, C. Mapping population distribution in the urban environment: The cadastral-based expert dasymetric system (CEDS). *Cartogr. Geogr. Inf. Sci.* **2007**, *34*, 77–102. [CrossRef]
73. Messager, M.L.; Ettinger, A.K.; Murphy-Williams, M.; Levin, P.S. Fine-scale assessment of inequities in inland flood vulnerability. *Appl. Geogr.* **2021**, *133*, 102492. [CrossRef]
74. Hallisey, E.; Tai, E.; Berens, A.; Wilt, G.; Peipins, L.; Lewis, B.; Graham, S.; Flanagan, B.; Lunsford, N.B. Transforming geographic scale: A comparison of combined population and areal weighting to other interpolation methods. *Int. J. Health Geogr.* **2017**, *16*, 1–16. [CrossRef]
75. Crowell, M.; Coulton, K.; Johnson, C.; Westcott, J.; Bellomo, D.; Edelman, S.; Hirsch, E. An estimate of the US population living in 100-year coastal flood hazard areas. *J. Coast. Res.* **2010**, *26*, 201–211. [CrossRef]
76. Cohen, D.T. 60 Million Live in the Path of Hurricanes. Available online: https://www.census.gov/library/stories/2018/08/coastal-county-population-rises.html (accessed on 16 September 2021).
77. Andersen, T.K.; Shepherd, J.M. A global spatiotemporal analysis of inland tropical cyclone maintenance or intensification. *Int. J. Climatol.* **2014**, *34*, 391–402. [CrossRef]
78. Yoo, J.; Santanello, J.A.; Shepherd, M.; Kumar, S.; Lawston, P.; Thomas, A.M. Quantification of the Land Surface and Brown Ocean Influence on Tropical Cyclone Intensification over Land. *J. Hydrometeorol.* **2020**, *21*, 1171–1192. [CrossRef]
79. Galarneau, T.J.; Davis, C.A.; Shapiro, M.A. Intensification of Hurricane Sandy (2012) through extratropical warm core seclusion. *Mon. Weather Rev.* **2013**, *141*, 4296–4321. [CrossRef]
80. Cutter, S.L. Vulnerability to environmental hazards. *Prog. Hum. Heography* **1996**, *20*, 529–539. [CrossRef]